Hadley Centre Technical Note – HCTN 12
January 2000

Differential changes in observed surface and atmospheric temperature since 1979

Simon Brown, David Parker and David Sexton
Hadley Centre for Climate Prediction and Research, The Met. Office, Bracknell, U.K.

Abstract

We analyse variations of temperature trends with height from the surface to the lower stratosphere using radiosonde, Microwave Sounding Unit (MSU), land and ocean surface air temperature and sea surface temperature (SST) data for 1979-1998. The profiles of trends are, in general, not sensitive to the version of gridded radiosonde temperature data set used, to collocation of the MSU and surface data to the sparser radiosonde data network, or to the choice of using fixed-pressure versus fixed height trends. Trends of difference series between atmospheric and surface temperatures can be more precisely specified than individual trends, because the subtraction removes common variance resulting from the El Niño – Southern Oscillation (ENSO) and other large-scale phenomena. These trends of temperature differences are only modestly affected by prior elimination of ENSO and volcanic influences.

Combined land surface air temperature and SST data and MSU lower-tropospheric temperature data for the tropics are fitted using restricted maximum likelihood (REML) and ordinary least squares (OLS) techniques to estimate intercept, trend, ENSO and volcanic components. More variance is explained by the predictors using OLS than REML, which uses a first order autoregression assumption, as REML can treat most of the ENSO component as red noise and does not allocate it to ENSO. However, as REML produces residuals which are consistent with the statistical model, it is considered that REML provides a better parameter estimate. This difference in performance is slightly reduced when (MSU lower troposphere temperature minus surface temperature) series are fitted, because of the removal of common anomalies with significant serial correlation thereby reducing the serial correlation in the remaining difference. Separate removal of ENSO and volcanic effects before subtracting the tropical series has more effect if done on a gridpoint-by-gridpoint basis rather than en bloc, because of the geographical variations of temperature-ENSO relationships in particular. When a series of tropical MSU mid- minus lower-tropospheric temperature is fitted, the relative warming trend of the former remains despite the allowance for ENSO and volcanoes in the fitting process, irrespective of whether REML or OLS is used.

Simultaneous fits of intercept, trend, ENSO and volcanic influences to MSU lower-tropospheric temperature minus surface temperature were also made using REML on a gridpoint by gridpoint basis. As expected, the results show a pervasive relative cooling trend in the lower troposphere in the tropics. The ENSO influence on the temperature difference shows large-scale coherence, with major areas of opposing sign. The volcanic

influence promotes relative cooling of the lower troposphere, even in the extratropics. Explanations for some of these findings are discussed.

1. Introduction

The differing temperature trends observed at different levels in the atmosphere provide key information for the understanding of climatic variations and the detection and attribution of climatic changes (Tett et al., 1996; Santer et al., 1996). However, they may also be affected by inadequacies in the global observing system, both surface-based (Karl et al., 1994), radiosonde (Gaffen, 1994; Gaffen et al., 1999), and satellite based (Hurrell and Trenberth, 1996, 1997; Wentz and Schabel, 1998). Part of our aim in this paper is therefore to assess the influence of the choice of data and analysis techniques on estimates of temperature trends. In addition, the trends, particularly when estimated over the short period for which satellite data are available, are susceptible to the influence of "noise" from short-term natural influences such as the El Niño – Southern Oscillation (ENSO) and volcanic eruptions (Christy and McNider, 1994; Jones, 1994b; Santer et al., 1999b). So we use a refined statistical technique to provide independent optimal estimates of trends and the influences of ENSO and volcanoes, both for temperatures at given levels from the surface to the lower stratosphere, and for temperature differences between the lower troposphere and the surface and between the mid- and lower troposphere. Our analysis looks at both the large scale (quasi-hemispherical) down to the gridscale influence of such factors.

2. Data and Methodology

2.1 Radiosonde data.

We use updated versions of the Hadley Centre Radiosonde Temperature (HadRT) data sets described by Parker et al. (1997). In summary:

HadRT2.0 is a monthly analysis, on a 5^{o} latitude x 10^{o} longitude grid, of standard-level (850 through 50 hPa) temperature anomalies relative to 1971-1990 climatology, and has no bias adjustments. Data sources are monthly telecommunicated "CLIMAT TEMP" messages, supplemented by some data published or provided on request by National Meteorological Services. Limited quality control has been performed e.g. hydrostatic checks

HadRT2.1 is the same as HadRT2.0 but with bias-adjustments to many data worldwide for 1979 onwards using the Microwave Sounding Unit (MSU) lower tropospheric retrieval MSU2LT version c and the lower stratospheric retrieval MSU4 (see Section 2.2) as a reference. Bias adjustments were only applied in cases of known changes of radiosonde instrumentation or operation. HadRT2.1s has adjustments at stratospheric levels (150hPa through 50hPa) only, based on MSU4.

HadRT2.2 contains seasonal and annual (not monthly) fields on a 10^{o} latitude x 20^{o} longitude resolution created by an eigenvector-based reconstruction of HadRT2.1. Higher order eigenvectors, taken to represent noise and biases, are excluded from the reconstruction resulting in approximately 78% of the original variance being retained. Grid boxes with no data are filled if

>= 2/3 of data is present. Some extra quality-controls, and an extension of the data over Antarctica, were carried out (Parker et al., 1997). HadRT2.2s has adjustments at stratospheric levels (150hPa through 50hPa) only, based on MSU4(see comment above re this), and HadRT2.2u is unadjusted. HadRT2.0 through 2.2 all have missing indicators in gridboxes with no data, i.e. even HadRT2.2 is not interpolated so as to be globally complete.

HadRT2.3 is globally complete. It is based on HadRT2.1, but with missing data filled using the Laplacian of the monthly average standard-level temperatures from the NCEP Reanalysis (Kalnay et al., 1996).

Due to the heterogeneous nature of Indian radiosonde data, this data was removed from all radiosonde data used here.

2.2. Microwave Sounding Unit data

The production of mid-tropospheric temperatures, MSU2, is documented by Spencer and Christy (1992a). The lower tropospheric retrieval (formerly MSU2R, now known as MSU2LT) is described by Spencer and Christy (1992b) and the lower stratospheric retrieval MSU4 is documented by Spencer and Christy (1993). Version c of MSU2LT, used for the adjustments to the HadRT data sets, is documented by Christy et al. (1998) and version d, which we have used in our trend analyses and time series, is described by Christy et al. (1999). Version d includes adjustments for the effects of orbital decay (Wentz and Schabel, 1998) , improved calibration coefficients and adjustments for the diurnal cycle and for the temperature of the instruments.

We calculated equivalent MSU temperatures from the standard level radiosonde temperatures using geographically-invariant weighting functions for MSU2 (Spencer and Christy, 1992a), MSU2LT (Spencer and Christy, 1992b) and MSU4 (Spencer and Christy, 1993), as described in the Appendix of Santer et al. (1999a). As the majority of the signal for MSU2LT comes from the lower troposphere only, the levels 850hPa through 300hPa were used. A surface contribution was included in the MSU2LT simulation with surface temperatures from JONES/MOHSST (see below) and assuming 20% (10%) of detected radiance comes from land (ocean). All relevant levels were required to be present for a simulated MSU temperature to be calculated

2.3. Surface temperature data

Land surface air temperatures, relative to 1961-1990 climatology, ("JONES") were taken from the Jones et al. (1999) update of the monthly Jones (1994a) data set. Sea surface temperatures ("MOHSST") were extracted from the monthly Meteorological Office Historical Sea Surface Temperature data set MOHSST6 (Parker et al., 1995) and marine air temperatures ("NMAT") extracted from the monthly Meteorological Office Historical Marine Air Temperature data set MOHMAT5 (Rayner et al., 1999a; Rayner et al., in preparation). Night-time air temperatures were used, to avoid biases arising from solar heating of ships' decks (Parker et al., 1995). "JONES/MOHSST" is a blend of "JONES" and "MOHSST" such that 5^{o} latitude x 5^{o} longitude grid boxes with both types of data were accorded a weighted average of each type, according to the proportion of land and sea, subject to minimum (maximum) weightings of 0.25 (0.75) to preserve

the influence of valuable, remote island data and of marine data near poorly-observed tropical land areas. All the marine data were available as differences from 1961-1990 climatology.

2.4 Methodology and statistical procedures

Two regression procedures were used. The first is ordinary least squares (OLS) and the second is the Restricted Maximum Likelihood method (REML), an adaptation of the Maximum Likelihood method that produces unbiased regression estimates (Diggle et al., 1994). The second method was employed to explicitly account for serial correlation in the noise, which is present in the data used in this study. The REML procedure applies weighted least squares regression estimation (Draper and Smith 1966) to determine regression parameters for a given serial correlation. Through iteration, a set of parameters (intercept, trend, ENSO coefficient, volcano coefficient, serial correlation) are chosen which maximises the REML likelihood function. Confidence intervals are calculated at the 95% level from the weighted least squares regression.

We focus on the period 1979 to 1998 where MSU data are available. We have selected four regions for analysis: Global (GL), Northern Hemisphere north of 20^{o}N (NH20), Tropics 20^{o}N-20^{o}S (TR) and the Southern Hemisphere south of 20^{o}S (SH20). Anomalous temperature time series are calculated from the described data by first calculating 5° latitude band averages and then averaging these, weighted by cosine latitude. This was found by Hurrell et al. (1999) to provide the best agreement between radiosonde and MSU data for such regional averages. All anomalies have been re-referenced to the period 1979-1998, the period of available MSU data.

3. Results

3.1 Temperature trend profiles of the atmosphere

The HadRT radiosonde data allow temperature trends to be determined at standard pressure levels through the depth of the atmosphere up to 50 hPa. In this section, we calculate trends for each standard level , MSU channel and surface data using the REML procedure.

3.1.1 Differences between HadRT products

Radiosonde data are well known for their deficiencies, particularly the heterogeneities introduced by changes in radiosonde instrumentation (Gaffen 1994, Parker and Cox 1995, Parker et al., 1997, Gaffen et al., 1999). So we first compare the different HadRT products, some of which have bias adjustments (Section 2.1), in terms of temperature trends since 1979 (Figure 1a). As HadRT2.2 and HadRT2.2u are only available as seasonal data, the other data are converted to seasonal resolution before trends are calculated. The differences between the HadRT versions are largest in the stratosphere because radiosonde instrumental biases increase with height: the unadjusted versions show greater cooling (Parker et al., 1997, Gaffen et al.,1999). The net effect of such instrumentation biases on tropospheric trends is small. Differences between products are smaller than the uncertainty in trends for all levels. For the globe, the unadjusted HadRT2.0 has consistently warmer trends than the other versions in the mid- and upper troposphere: this mainly arises from the extratropical Southern Hemisphere. The eigenvector filtered data have consistently cooler trends in the troposphere, especially in the tropics, though differences are small. The difference between the adjusted and unadjusted eigenvector filtered data (HadRT 2.2

& HadRT 2.2u) are very small for the lowest levels, suggesting that eigenvector filtering is removing the majority of the biases relative to MSU. This might be expected as a discrete jump introduced by one station changing radiosonde type would describe little of the total variance and thus appear in a high order eigenvector and be omitted. A more direct application of this effect for bias adjustment is being pursued for a new HadRT product. The eigenvector filtered products have uncertainty estimates which are ~10% smaller than those for HadRT2.0, owing to the removal of high frequency variance by filtering. It can be seen that for TR and SH20, where the radiosonde data coverage is less complete, the inclusion of reanalysis data in HadRT2.3 can alter the trends away from the unblended data. Potential causes for this result are discussed later.

3.1.2 Radiosonde temperature trends relative to surface trends

Temperature trends for HadRT2.1s are plotted in Fig. 1b together with trends for JONES, MOHSST, JONES/MOHSST, NMAT and the MSU. All available data are used. For all regions the general structure is the same with the surface trends somewhat warmer than those of the lower troposphere. The troposphere shows a relatively constant temperature trend up to 300 hPa, that differs somewhat between region, and the stratosphere shows an increased cooling with height. The major differences between the regions are the warming of the NH20 troposphere compared with tropospheric cooling in TR and SH20 to 500hPa, though at 300 hPa where there is an indication of slight warming. This upper tropospheric warming relative to the lower troposphere is also seen between MSU2LT and MSU2, but all these relative differences are less than the errors plotted. The surface trends show warming relative to the troposphere for all regions, with the greatest relative warming in TR as previously found by many authors (Hurrell and Trenberth, 1996, 1997; Balling, 1996; Jones, 1994b; Jones et al., 1997, Christy and Mcnider, 1994). Note that the NMAT trends are intermediate between the other surface trends and the 850 hPa trends for all regions other than SH20 where the NMAT data are very sparse. Furthermore the 850 hPa layer shows warming relative to the 700 hPa level in the radosonde data except in SH20. The MSU trends are plotted at pressures which correspond to the level from which the greatest radiance is received by the satellite for each of the products, although it should be noted that each product receives radiation from a thick layer of the atmosphere, particularly MSU2. Corresponding simulated MSU trends from HadRT2.1s data are also plotted. It can be seen that the agreement between the MSU and the radiosonde trends is generally very good. The largest differences are in the lower stratosphere where MSU shows somewhat less cooling. This may be a result of unadjusted biases at radiosonde stations with insufficient metadata to allow adjustments to be made (Parker et al., 1997) but the differences are within the 95% uncertainty of the trend estimates. The largest difference in the troposphere is in the tropics for MSU2 which shows relative warming, although again this is within the trend uncertainty.

3.1.3 Effect of coverage on trends

Collocation of radiosonde and MSU data has little effect on the general nature of the profiles of temperature trends, as can be seen from Fig. 1c where HadRT2.3s, MSU and surface trends are shown both for the spatially complete analysis and after collocation to HadRT2.0. In general, collocation cools radiosonde tropospheric trends for all regions and warms stratospheric trends. The cause of this systematic biasing is uncertain. The largest change is seen with SH20, where the radiosonde coverage is the most sparse. There are two possible explanations. Firstly, regions not sampled by the radiosonde network are experiencing systematic warming in the troposphere and cooling in the stratosphere. Secondly, the influence of reanalysis model biases

have not been completely removed from the blended HadRT2.3 data set. Large biases were found in the reanalysis atmospheric temperatures relative to the radiosonde data prior to blending (see also Santer et al., 1999a) which suggests this as the more likely explanation for the differences seen in Fig. 1c.

3.1.4 Change in height of pressure levels

Trends calculated at fixed pressure levels are influenced by the geopotential height changes resulting from temperature changes at layers below, so they may differ from trends calculated at specific heights. Warming (cooling) beneath a given fixed-pressure surface will, other things being equal, raise (lower) its geopotential height. This will result in cooling (warming) at fixed-pressure surfaces, compared with nearby fixed-geopotential surfaces. The influence of such effects is depicted by the differences between the red (fixed height) and black (fixed pressure) temperature trends in Fig. 1d. The greatest adjustments are for upper levels particularly the stratosphere where the global average cooling at 50 hPa is increased by 0.17 °C /decade by using fixed height. For the lower troposphere the adjustments to the trends are small, no more than 0.04 °C /decade but more usually ~0.01 °C /decade so this effect can be neglected for trends over this period. For comparison with MSU the fixed pressure calculations are appropriate, but the calculation shows that in the stratosphere this method slightly underestimates the equivalent fixed level cooling seen since 1979.

3.1.5 Trends in difference from surface temperature

The differences between trends discussed in this section have, on the whole, been small relative to the uncertainty in the trend estimates as shown by the 95% error bars in the figures. There are two principle additional factors which inflate the uncertainties and preclude more definitive results (Santer et al., 1999b). The first is the influence of ENSO on temperature. ENSO has a high serial correlation, resulting in a large noise term in the regression and hence large uncertainties. Secondly, much of the variability, such as that due to ENSO, is common between tropospheric levels and the surface. This means that although the absolute uncertainty in the trend for a given level is large, the relative uncertainty to that in another level is much smaller. This can be partially eliminated by calculating temperature trends of the differences between two levels. In Fig. 1e, data have been subtracted from JONES/MOHSST surface temperatures and trends in the differences calculated. Uncertainty estimates for trends in these differences are much smaller than those for the trends at individual levels. This is not true for the stratosphere where interannual temperature variations are not positively correlated with those at the surface. The surface minus tropospheric temperature difference trends are all significantly different from zero for all regions except SH20. This is in accord with the results of Santer et al. (1999b). The NMAT warming trends are found to be significantly less than those of Jones/GISST for the Globe, Tropics and SH20, although NMAT data for SH20 are questionable (Section 3.1.2).

Figure 1e also shows that the TR (surface minus MSU2) temperature difference trend is less positive than the corresponding difference trend using MSU2LT (although within uncertanty), whereas this is not true for the other regions. Otherwise, as the surface is approached the trends in the difference tend towards zero, suggesting that tropospheric trends well away from the surface are genuinely different from those at the surface.

The surface minus tropospheric temperature trends are an approximate measure of trends in lapse rate (albeit in a negative sense). Strictly speaking lapse rate is -dT/dz whereas the difference used above is dT/dp, but Fig. 1d suggests that the error associated with assuming dp and dz are equivalent is small as discussed in Brown et al. (2000).

3.2 The influence of ENSO and Volcanoes on atmospheric and surface temperature trends.

3.2.1 Temperature anomaly time series

Surface and atmospheric temperatures are known to be strongly influenced by El Nino/ La Niña oscillations and volcanic eruptions (Christy and McNider, 1994; Jones, 1994b). These studies aimed to remove such effects through linear regression on individual surface and MSU2LT time series before performing trend analyses. They led to the conclusion that much of the difference in temperature trends between the surface and the troposphere can be explained by these factors. We have performed a similar analysis for data up to 1998 (rather than 1993), but using the REML regression procedure, which accounts for serial correlation, to fit intercept, linear trend, ENSO and volcanic terms simultaneously. By regressing in this way uncertanties in the trends take account of the uncertanties in the estimates of the other terms. The results are presented in Table 1. This contains coefficients for trend, ENSO and volcanic effects, r^2 values, number of months the ENSO and volcanic indices were delayed in the regression, and the serial correlation determined from the regression procedure.

We used the Niño 3 region (5^oN-5^oS, 90^oW-150^oW) SSTs as an ENSO index and the volcanic dust veil index updated from Sato et al. (1993). Christy and McNider (1994) developed an empirical function to describe the influence of volcanoes on atmospheric temperature but we found no significant difference between these two approaches. Different parts of the world respond on different time scales to both ENSO and volcanic eruptions (Halpert and Ropelewski 1992). To allow for this on a global or regional average, each of the indices were delayed by up to 12 months independently and the regression recalculated (using ordinary least squares to reduce computation time). The pair of shifts which provided the smallest sum of squared residuals were then used to determine the regression coefficients in Table 1 using REML regression. For tropospheric radiosondes (850 hPa to 150 hPa) an average temperature was used to determine the appropriate shift as the individual pressure level temperatures produced erratic shifts relative to other layers.

Our results do not convincingly show that ENSO and volcanoes account for the difference in temperature trends between the surface and the lower troposphere over this period. These surface and MSU2LT trends for the global domain do not agree within 95% confidence limits, in disagreement with Christy and McNider (1994). In the tropics the MSU2LT trend is consistent with that at the surface but this appears to be due to the large uncertanty in the tropical MSU2LT trend. In contrast the tropospheric radiosonde trends do significantly differ from the surface. There appear to be two factors contributing to these inconclusive results. First, as mentioned in the previous section, ENSO exhibits considerable serial correlation, a significant fraction of which can be described by a first order autoregressive process. Thus the regression procedure has the option of “allocating” the variability due to ENSO to noise which results in increased uncertainty in

the regression coefficients, or assign it to the ENSO coefficient. Both appear to have taken place in Table 1. The tropical ENSO coefficient for MSU2LT is considerably smaller but the trend uncertainty is considerably larger than that for the global MSU2LT. This is surprising as ENSO has the greatest influence on atmospheric temperatures in the tropics. Similarly for tropical MOHSST the regression sets a very small ENSO coefficient, even though ENSO dominates the tropical SST variability. To illustrate this we performed the same regression procedure for tropical MOHSST but without accounting for auto-regressive noise, i.e. ordinary least squares multiple regression, with the result labelled MOHSST(ols) in Table 1. Now the ENSO coefficient is much larger and the trend uncertainty smaller, but the trend value has stayed the ***same*** i.e. irrespective of the regression procedure and the method of accounting for ENSO, the trend is found to be robust. This illustrates a tension between determining the "best" statistical fit and the largest variance (as described by the explanatory variables) with the REML providing the first and OLS the latter in this case.

3.2.2 Differential effects of volcanoes and ENSO between atmosphere and surface

The second factor contributing to the inconclusive results in Table 1 is that there is considerable variability in the surface and tropospheric temperature which is not due to ENSO or volcanoes but is still correlated between the different series. So we have repeated the regressions but using the difference of each series from the JONES/MOHSST series (Table 2) as before. Shifts for the tropospheric radiosondes were only calculated from the average temperatures from levels 700 hPa to 150 hPa as the 850 hPa layer was found to show different characteristics from the other tropospheric levels. The majority of the regression parameters for ENSO and volcanoes are significant at the 95% level, confirming the differential response to ENSO and volcanic eruptions of layers in the atmosphere with respect to the surface. However, the majority of trend coefficients are also significant indicating that the atmosphere and surface temperature trends are different, particularly for the tropics, irrespective of their differential responses to ENSO and volcanic eruptions.

Trends from Table 2 are plotted in Figure 1f, together with trends from the simple linear regression of Figure 1e where ENSO and volcanic effects have not been modelled. Figure 1g is as for Fig. 1f except OLS regression has been used rather than REML. Accounting for the effects of ENSO and volcanoes has little impact on the general vertical structure of these trends in temperature differences from JONES/MOHSST, irrespective of regression method. The largest change is seen for NH20 where there is a general increase in trends for most pressure levels, although within trend uncertainties. These results indicate that differencing the two temperature series has virtually eliminated the effects of ENSO and volcanoes on *trends*, even though there are still significant ENSO and volcanic influences on the timeseries.

3.2.3 Differential effects of volcanoes and ENSO within the atmosphere

Tables 1 and 2 show that different layers of the atmosphere respond to ENSO and volcanoes in varying degrees. There is a tendency for the influence of ENSO at a given level, relative to JONES/MOHSST, to become more positive the closer to the tropopause (e.g. 200 hPa) for all regions except for NH20. The increased influence of ENSO with height is consistent with the atmospheric response to a surface temperature anomaly, particularly for TR, being a combination

of dry and moist processes[1]. This is not the case, however, for the lowest layer of TR where the TR JONES/MOHSST minus 850 hPa ENSO coefficient is positive showing that the tropical surface warms more than the corresponding 850 hPa layer**.** The tropospheric cooling response to volcanoes also appears to generally increase with height, particularly for TR, with the atmosphere cooling more than the surface which is again consistent with an adiabat where moisture plays a role in the atmospheric response to surface anomalies. This is not the case in the stratosphere where there is a strong warming following a volcanic eruption as documented in detail by many authors, e.g. Spencer and Christy (1993). Note that the volcanic coefficients change from cooling to warming relative to the surface between 150 and 100 hPa for all regions, whereas this change in sign for ENSO effects occurs between 100 and 50 hPa (although only significantly for GL). This difference is not yet fully understood. The levels at which volcanic warming occurs are likely to be determined by the levels at which the volcanic aerosol resides, which are expected to vary from eruption to eruption. However there may not be a one-to-one relationship (Angell, 1997), because the heating will affect atmospheric dynamics (McCormick et al., 1995).The boundary between ENSO-related warming and cooling is likely to be determined by atmospheric dynamics consequent on the anomalous flow patterns, which are wavelike in the extratropics: for a review see Trenberth et al. (1998).

A further study was performed on the differential response within the atmosphere for the TR region. Regressions were calculated on differences with respect to 850 hPa temperatures (Table 3). The results are qualitatively similar to those in Table 2 with trends in the temperature differences steadily becoming more positive with height, although the trends of the differences for the lowest levels are not significant due to their small value. The ENSO coefficient is marginally most negative for the 100 hPa difference, with little change in the coefficient in the 300hPa to 100hPa layer, much as in Table 2. The positive coefficient for the 50 hPa difference is now significant. The volcanic results are also similar to those in Table 2 except that the tropospheric coefficients peaks now with the 300 hPa difference rather than with the 150 hPa difference. The different levels at which coefficients for ENSO and volcanic effects change sign are as in Table 2.

3.2.4 Sensitivity to ENSO and volcanic time shifts

The influences of ENSO and volcanic eruptions on temperature are delayed by differing amounts for the surface, layers within the atmosphere and for different regions. This was accounted for in the regression procedure by shifting in time the ENSO and volcanic indices independently by up to 12 months and recalculating the regression. Ordinary least squares regression was used and the shifts which resulted in the smallest sum of squared residuals were chosen. This reduced computation time and produced a smoother sum of squared residual distribution facilitating finding the minimum. The optimum shifts are given in Tables 1 and 2. The value of shift for both ENSO and volcanic effects does not give any particular physical insight, and there is no clear pattern between different series or atmospheric levels. The sensitivity of the regressions to the shift values chosen was determined by specifying ENSO and volcanic shifts at 0,4,8 and 12 months and re-calculating the regression. Data used were Jones/MOHSST minus MSU2LT and the results are presented in Table 4. The trend in temperature differences is very insensitive to the shift value. The coefficients for ENSO and volcanoes are both sensitive, however, justifying

[1] If a purly moist adiabat were followed then the corresponding ENSO coefficients would be 0.06, 0.10, 0.40 and 1.2 for 850, 700, 500 and 300 hPa respectively.

the inclusion of optimum shifts in the regressions. One factor which contributed to the robustness of the trend but not its value is the removal of the first order effects of ENSO and volcanoes by the differencing process.

3.2.5 Statistical and Physical models

We analysed in more detail some of the regressions within Table 1 and 2 to enhance understanding of the results from the different statistical and physical models. Figures 2a to d are the graphical representation of the fits of trends, ENSO and volcanic effects for Jones/MOHSST and MSU2LT respectively for the tropics, a) and c) using OLS and b) and d) using REML. Figures 3 a) and b) are the equivalent plots for JONES/MOHSST minus MSU2LT differences, henceforth referred to as JMLT. Table 5 contains corresponding parameters from the regression procedure. As previously mentioned, there can be considerable differences between the OLS and REML treatment of ENSO, with the REML deriving a small ENSO coefficient and a large serial correlation and therefore attributing much of the variability in the time series to noise. As a result, the variance of the REML fit (see VOF in Table 5) is considerably smaller than that for OLS, and there is a relatively poor description of the observed variance (e.g. r^2 values of 0.08 compared with 0.89 for the surface). However, although the OLS regression may describe a larger fraction of the variance, or be a good 'predictor', the quality of the final statistical fit is poor relative to REML and consequently less likely. This can be shown by the spectrum of the OLS residuals (bottom panel REV 1a and 2a) deviating strongly from the theoretical spectrum assumed by the regression (dashed lines) whereas those for REML, 1b) and 2b) are in good agreement with the theoretical spectrum. This is because the latter takes formal account of autoregression in the data.

By contrast, Figs. 3 a) and b) show that OLS and REML produce very similar fitted time series when using JMLT differences, returning r^2 values of 0.79 and 0.57 respectively (Table 5). The removal of common variance by differencing has also reduced the serial correlation of JMLT to 0.45 compared with 0.92 and 0.86 for Jones/MOHSST and MSU2LT respectively. However, it is possible that differencing prior to the regression has had undesirable effects. We have already mentioned that the atmosphere and surface have different response times to ENSO and volcanic eruptions so differencing with no relative time shift between the surface and the atmosphere could introduce a complex net effect. To investigate this, OLS regression, with optimum shift, to remove just ENSO and volcanic effects from the individual temperature time series was performed prior to differencing. REML regression was then performed, as for REV 3b), on this modified difference. The results, Fig. 3c), show that this two stage regression has had very little effect on the derived coefficients but has increased residual errors and reduced the r^2 value. The atmospheric or surface response to ENSO and volcanoes may also vary in time and magnitude across the tropics. To test this, the linear effects of ENSO and volcanoes were removed through OLS regression on a gridpoint by gridpoint basis. Shifts calculated from individual gridpoints were found to be spatialy noisy so a simple 1:2:1 smoothing was applied North-South and East-West. Tropical mean temperature time series and JMLT were then calculated in the usual way and REML regression performed. The results (Fig. 3d), show that most of the ENSO and volcanic effects have been removed with coefficients for these being much smaller than in Figs. 3a-c. The trend in the difference is still of the order of 0.2 °C/decade. The red residuals of this regression are the most "white" of all the regressions using JMLT although there appears to be a strong annual cycle in the time series. This may have arisen from differences between the

annual cycles in the MOHSST and JONES 1961-1990 climatologies and the average annual cycles over the 1979-1998 period under study for the tropics. Alternatively, there may be biases in these or the MSU climatology. The small magnitudes of the whitened residuals in Fig. 3d, however, show that these biases are very small. The r^2 value for the regression in Fig. 3d (0.25) is smaller than some of the r^2 values for the other regressions, but this should not be interpreted as indicating that Fig. 3d is a poorer fit as the input data are not identical. For 3d a considerable amount of the variance not due to noise has been removed by the prior elimination of ENSO and volcanic effects, and therefore it should not be expected to have as high an r^2 value. However, it does have the smallest mean squared error of all the regressions using JMLT (Table 5).

3.2.6 MSU2 vs. MSU2LT

There has been some concern that MSU2 has a considerably warmer trend in the tropics than MSU2LT, (Hurrell and Trenberth, 1998; Figure 1b) as the combination of a warming surface, non-warming or cooling lower troposphere (MSU2LT) and a warming upper troposphere (MSU2) is physically difficult to explain. This has been taken as an indication that some of the MSU temperatures may be in error. To assess the difference between MSU and MSU2LT in terms of ENSO and volcanic effects, OLS and REML multiple regressions were performed on tropical MSU2LT minus MSU2 temperature differences (Figs. 4a and b) Although there is a significant differential response to volcanoes the temperature trend between the two measures is found to be robust at 0.07 °C/decade.

3.3 Small scale trends, ENSO and volcanic effects

In the previous sections, we have assessed the influence of ENSO and volcanic eruptions on large scale temperatures. Here we examine the small scale response of JMLT differences to such events. Similar regressions (to Fig. 3b) were performed on gridded JMLT data from 70°N to 70°S. For individual gridpoints the best shift in time for the ENSO and the volcanic indices was calculated as before followed by the multiple regression. The results are presented in Figs. 5 a) to c). Upper panels show results for grid boxes with <30% data missing; the lower panels show grid boxes where the fitted component is significant at the 95% level.

3.3.1. Regional trends in JMLT.

For comparison with Fig. 5a, trends from REML regression fitting just trend and intercept are plotted in Fig. 5d. The temperature trend maps are very similar for the two regression approaches with much of the domain indicating a warming of the surface relative to the atmosphere, particularly for the tropics.

3.3.2 Regional ENSO response in JMLT

Figure 5b shows the gridded ENSO coefficients (upper panel) and those which are significant at 95% (lower panel). The ENSO influence on JMLT is found to be highly spatially variable, but nonetheless shows considerable spatial coherency. The major response of JMLT to ENSO is twofold. First, there is a strong positive response (tropospheric warming less than at surface) along the equatorial Pacific, east of the date line corresponding to the strong ENSO SST anomalies. This positive response extends to the North American west coast and land mass, and from the Gulf of Alaska across the far northern Pacific and down the western Pacific almost to the

equator. There is a hint that an equivalent pattern is repeated in the Southern Hemisphere but sufficient data are not available for much of the Southern Pacific. In contrast, immediately north and south of the strong equatorial Pacific positive response are large negative coefficients (troposphere warming more than surface). These cover much of the remainder of the Pacific. The other ocean basins also have a weaker negative response. The response over Eurasia is more mixed with little being found to be significant. Those which are, are predominantly positive (surface warming greater than atmosphere), mainly in the Asian monsoon region. Inasmuch as El Nino tends to relate to a weakened Indian monsoon (e.g. Navarra et al., 1999), this is an expected result: reduced convection yields a cooler troposphere while reduced cloud yields a hotter surface over the land.

3.3.3 Regional Volcanic response in JMLT

The volcanic response Fig. 5c is more uniform than the ENSO response with the majority of the domain showing a positive relationship i.e. atmosphere cooling more than the surface. This is to be expected in the tropics, and maybe over the summer continents, with the tropospheric temperature anomalies approximately following a combination of moist and dry adiabats. However the same relation cannot be expected in other regions and seasons. Part of the reason for the more negative negative coefficients seen in the Northern Hemisphere may be that, following major tropical volcanic eruptions, the resulting anomalous meridional stratospheric temperature gradients, with the tropical stratosphere anomalously warm, are conducive to enhanced tropospheric westerly flow (Robock and Mao, 1992; Kelly et al., 1996; Parker et al., 1996). This results in mild winters over Eurasia, with weakened surface inversions. These effects have also been reproduced in models (Graf et al., 1994).

4. Discussion

The geographical variations of the ENSO influence on lower tropospheric lapse rates highlights the need to maintain and improve the Global Climate Observing System (GCOS), especially the GCOS Upper Air Network (GUAN) of radiosonde stations (Wallis, 1998; Folland et al., 1999), in order to monitor, reliably, changes in lapse rate in regional, interannual detail. This will support both the understanding and prediction of interannual changes in the ocean-atmosphere-land system as targeted under the “GOALS” stream of CLIVAR (ICSU / WMO / UNESCO, 1999). Neither the radiosonde network nor the MSU retrievals can do this alone: the detailed vertical resolution of the radiosondes must be complemented by the geographical completeness of MSU.

Nonetheless, Fig. 5a shows that, when the influences of ENSO and volcanoes have been taken into account, there remains a pervasive increase in the lower tropospheric lapse rate in the tropics, subtropics and some higher latitude areas. This implies that radiosonde-based trends over decadal and longer periods are likely to be representative of larger areas than the radiosonde-based anomalies for months or seasons used by Wallis (1998) to design a network for climate monitoring and analysis. This finding also underlines the discovery by Brown et al. (2000) that interdecadal changes in lapse rate, measured by radiosondes since the late 1950s, have been coherent between different sectors of the tropics wherever reliable radiosonde stations are available.

5. Conclusions

Our analyses of temperature trends with height from the surface to the lower stratosphere, using radiosonde, MSU, and *in situ* surface data for 1979-1998, show that the implied increase of lapse rate for the tropics and the globe is robust to the version of gridded radiosonde temperature data set used, to collocation of the MSU and surface data to the sparser radiosonde data network, or to the choice of using fixed-pressure versus fixed height trends. The increased lapse rate may have been caused in part by natural multidecadal changes of atmospheric and oceanic circulation (Hurrell and Trenberth, 1996; Brown et al., 2000) and by anthropogenic forcing through stratospheric ozone loss (Hansen et al., 1997). However, the lapse rate changes may also be partly spurious, owing to remaining heterogeneities in the surface, radiosonde and MSU temperature records, despite ongoing attempts to improve them. Notwithstanding, we have shown that ENSO and volcanic influences have not made substantial contributions to the lapse rate trends since 1979.

Our results demonstrate the need for ongoing maintenance and improvement of the Global Climate Observing System, especially its radiosonde network.

References

Angell, J.K., 1997: Stratospheric warming due to Agung, El Chichón, and Pinatubo taking into account the quasi-biennial oscillation. J. Geoph. Res., 102, 9479-9485.

Balling, R. C., 1996: Geographic analysis of differences in trends between near-surface and satellite based temperature measurements. *Geophys. Res. Lett.*, **21**, 2939-2941.

Brown, S. J., D. E. Parker, C. K. Folland and I Macadam, 2000: Decadal variability in the lower-tropospheric lapse rate. Submitted to *Geophys. Res. Lett*.

Christy,J.R. and R.T.McNider, 1994: Satellite greenhouse warming. *Nature*, **367**, 325.

Christy, J. R., R. W. Spencer and W. D. Braswell, 1999: MSU tropospheric temperatures: dataset construction and radiosonde comparisons. *J. Atmos. Ocean. Tech.*, in press.

Christy, J. R., R. W. Spencer and E. S. Lobl, 1998: Analysis of the merging procedure for the MSU daily temperature series. *J. Climate*, 11, 2016-2041.

Diggle, P.J., K-Y. Liang and S. L. Zeger, 1994: *Analysis of Longitudinal Data*. Clarendon Press, Oxford, Chap. 4

Draper and Smith 1966: Applied regression analysis. John Wiley & Sons, New York

Folland, C. K., P. Frich, T. A. Basnett, N. A. Rayner, D. E. Parker, and E. B. Horton, 1999: Uncertainties in climate data sets – a challenge for WMO. Invited Scientific Lecture delivered by C.K. Folland to WMO Congress Cg-XIII, 21 May 1999. *WMO Bulletin*, in press (1999).

Gaffen, D. J., 1994: Temporal inhomogeneities in radiosonde temperature records. *J. Geophys. Res.*, **99**, 3667-3676.

Gaffen, D. J., M. A. Sargent, R. E. Habermann and J. R. Lanzante, 1999: Sensitivity of tropospheric and stratospheric temperature trends to radiosonde data quality. *J. Climate*, in press.

Graf, H.F., J. Perlwitz and I. Kirchner, 1994: Northern Hemisphere tropospheric mid-latitude circulation after violent volcanic eruptions. Beit. Phys. Atmos., 67, 3-13.

Halpert, M. S. and C. F. Ropelewski, 1992: Surface temperature patterns associated with the Southern Oscillation. *J. Climate*, **5**, 577-593.

Hansen, J., M. Sato, R. Ruedy, A. Lacis, K. Asamoah, K. Beckford, S. Borenstein, E. Brown, B. Cairns, B. Carlson, B. Curran, S. de Castro, L. Druyan, P. Etwarrow, T. Ferede, M. Fox, D. Gaffen, J. Glascoe, H. Gordon, S. Hollandsworth, X. Jiang, C. Johnson, N. Lawrence, J. Lean, J. Lerner, K. Lo, J. Logan, A. Luckett, M.P. McCormick, R. McPeters, R. Miller, P. Minnis, I. Ramberran, G. Russell, P. Russell, P. Stone, I. Tegen, S. Thomas, L. Thomason, A. Thompson, J. Wilder, R. Willson and J. Zawodny, 1997: Forcings and chaos in interannual to decadal climate change, J. Geophys Res., 102, 25679-25720.

Hurrell, J. W. and K. E. Trenberth, 1996: Satellite versus surface estimates of air temperature since 1979. *J. Climate*, **9**, 2222-2232.

Hurrell, J. W. and K. E. Trenberth, 1997: Spurious trends in satellite MSU temperatures from merging different satellite records since 1979. *Nature*, **386**, 164-167.

ICSU/WMO/UNESCO, 1999: Proceedings of the International CLIVAR Conference, Paris, 2-4 December 1998. WCRP-108, WMO/TD No. 954, ICPO No. 27, 279pp.

Jones, P. D. 1994a: Hemispheric surface air temperature variations: a reanalysis and an update to 1993, *J.Clim*, **7**, 1794-1802.

Jones, P. D. 1994b: Recent warming in global temperature series, *Geophys. Res. Lett.*, **21**, 1149-1152.

Jones, P. D., M. New, D. E. Parker, S. Martin and I. G. Rigor, 1999: Surface air temperature and its changes over the past 150 years. *Rev. Geophys.*, **37**, 173-199.

Jones, P. D., T. J. Osborn, T. M. L. Wigley, P. M. Kelly and B. D. Santer, 1997: comparisons between the microwave sounding unit temperature record and the surface temperature record from 1979 to 1996: real differences or potential discontinuities?. *J. Geophys. Res.*, 102, 30135-30145.

Kalnay, E., M. Kanamitsu, R. Kistler, W. Collins, D. Deaven, L. Gandin, M. Iredell, S. Saha, G. White, J. Woollen, Y. Zhu, M. Chelliah, W. Ebisuzaki, W. Higgins, J. Janowiak, K. C. Mo, C. Ropelewski, J. Wang, A. Leetmaa, R. Reynolds, R. Jenne and D. Joseph, 1996: The NCEP/NCAR 40-year reanalysis project. *Bull. Amer. Meteor. Soc.* **77**, 437-471.

Karl, T. R., R. W. Knight, and J. R. Christy, 1994: Global and hemispheric temperature trends: Uncertainties related to inadequate spatial sampling*, J. Climate*, **7**, 1144-1163.

Kelly, P. M., P. D. Jones and J. Pengqun, 1996: The spatial response of the climate system to explosive volcanic eruptions. *Internat. J. Climatol.*, **16**, 537-550.

McCormick, M. P., L. W. Thomason and C. R. Trepte, 1995: Atmospheric effects of the Mt Pinatubo eruption. *Nature*, **373**, 399-404.

Navarra, A., M. N. Ward and K. Miyakoda, 1999: Tropical-wide teconnection and oscillation. I: Teleconnection indices and type I/Type II states. *Quart. J. Roy. Meteorol. Soc*., **125**, 2909-2935.

Parker, D. E. and D. I. Cox, 1995: Towards a consistent global climatological rawinsonde data-base. *Int. J. Climatol*., **15**, 473-496.

Parker, D. E., C. K. Folland and M. Jackson, 1995: Marine surface temperature: observed variations and data requirements. *Climatic Change*, **31**, 559-600.

Parker, D. E., M. Gordon, D. P. N. Cullum, D. M. H. Sexton, C. K. Folland and N. Rayner, 1997: A new gridded radiosonde temperature data base and recent temperature trends. *Geoph. Res. Letters*, **24**, 1499-1502.

Parker, D.E., H. Wilson, P. D. Jones, J. R. Christy and C. K. Folland, 1996: The impact of Mount Pinatubo on worldwide temperatures. *Int. J. Climatol.*, **16**, 487-497.

Rayner, N. A., C. K. Folland and D. E. Parker, 1999a: The Meteorological Office Historical Night Marine Air Temperature data set version 5 (MOHMAT5N), 1856-1998. *Hadley Cent*re *Internal Note* **88**.

Rayner, N. A., E. B. Horton, D. E. Parker, C. K. Folland and R. B. Hackett, 1996: Version 2.2 of the Global sea-Ice and Sea Surface Temperature data set, 1903-1994. *Hadley Centre Climate Research Technical Note* **CRTN 74**.

Robock, A. and J. Mao, 1992: Winter warming from large volcanic eruptions. *Geoph. Res. Lett*., **12**, 2405-2408.

Santer, B. D., J. J. Hnilo, T. M. L. Wigley, J. S. Boyle, C. Doutriaux, M. Fiorino, D. E. Parker, and K. E. Taylor, 1999a: Uncertainties in observationally based estimates of temperature change in the free atmosphere. *J. Geoph. Res*., **104**, 6305-6333.

Santer, B. D., T. M. L. Wigley, T. P. Barnett and E. Anyamba, 1996: Detection of climatic change, and attribution of causes. In *Climate Change 1995 - The Science of Climate Change. The second assessment report of the Intergovernmental Panel on Climate Change: Contribution of Working Group I.* J.T. Houghton, L.G. Meira Filho, B.A. Callander, N. Harris, A. Kattenberg and K. Maskell (Eds.). Cambridge University Press, Cambridge, UK, pp.407-443.

Santer, B. D., T. M. L. Wigley, J. S. Boyle, D. J. Gaffen, J.J. Hnilo, D. Nychka, D.E. Parker and K. E. Taylor, 1999b: Statistical significance of trends and trend differences in layer-average atmospheric temperature time series. *J. Geoph. Research*, in press (1999).

Sato, M., J. E. Hansen, M. P. McCormick and J. B. Pollack, 1993: Stratospheric areosol optical depths, 1850-1990. J. Geophys. Res., 98, 22987-22994.

Spencer, R. W., and J. R. Christy, 1992a: Precision and radiosonde validation of satellite gridpoint temperature anomalies, Part I: MSU channel 2. *J. Climate***, 5**, 847-857.

Spencer, R. W., and J. R. Christy, 1992b: Precision and radiosonde validation of satellite gridpoint temperature anomalies, Part II: A tropospheric retrieval and trends during 1979-90. *J. Climate*, **5**, 858-866.

Spencer, R. W., and J. R. Christy, 1993: Precision lower stratospheric temperature monitoring with the MSU: Validation and results 1979-91. *J. Climate*, **6**, 1194-1204.

Tett, S. F. B., J. F. B. Mitchell, D. E. Parker, and M. R. Allen, 1996: Human influence on the atmospheric vertical temperature structure: detection and observations. *Science,* **247**, 1170-1173.

Trenberth, K. E., G. W. Branstator, D. Karoly, A. Kumar, N-C. Lau and C. Ropelewski, 1998: Progress during TOGA in understanding and modeling global teleconnections associated with tropical sea surface temperatures. *J. Geoph. Res*., **103**, 14291-14324.

Wallis, T., 1998: A subset of core stations from the Comprehensive Aerological Reference Dataset (CARDS). *J. Climate*, **11**, 272-282.

Wentz, F. J. and M. Schabel, 1998: Effects of orbital decay on satellite-derived lower-tropospheric temperature trends. *Nature*, **394**, 661-664.

World Meteorological Organization, 1956 to 1999: International List of Selected, Supplementary and Auxiliary Ships. WMO No. 47, published annually and now in digital form.

ACRONYMS

CARDS	Comprehensive Aerological reference Data Set
CLIVAR	CLImate VARiability programme coordinated by ICSU/WMO/UNESCO.
ENSO	El Niño – Southern Oscllation
GCOS	Global Climate Observing System
GISST	Global sea-Ice and Sea Surface Temperature
GUAN	GCOS Upper Air Network (radiosonde)
ICSU	International Council of Scientific Unions
ICPO	International CLIVAR Project Office
MSU	Microwave Sounding Unit
OLS	Ordinary least Squares
REML	Restricted Maximum Likelihood
UNESCO	United Nations Educational, Scientific and Cultural Organization
WCRP	World Climate Research Program
WMO	World Meteorological Organization

Global	Trend	err	ENSO	err	Volcano	err	r^2	ENSO shift	Vol shift	Serial corr
JONES	**0.18**	0.06	**0.09**	0.03	**-2.99**	1.07	0.56	8	8	0.43
MOHSST	**0.16**	0.04	**0.04**	0.02	**-0.96**	0.69	0.60	4	7	0.66
NMAT	**0.05**	0.05	**0.04**	0.02	**-0.99**	0.86	0.51	4	9	0.57
MSU 2lt	0.04	0.06	**0.09**	0.03	**-3.36**	1.01	0.23	6	6	0.57
MSU 2	0.02	0.05	**0.10**	0.02	**-2.77**	0.85	0.28	7	10	0.51
MSU 4	**-0.51**	0.20	0.03	0.03	**8.15**	2.31	0.26	3	0	0.90
HadRT2.0_850	0.02	0.06	**0.07**	0.03	**-2.71**	0.96	0.32	7	11	0.34
HadRT2.0_700	-0.01	0.06	**0.09**	0.03	**-2.71**	1.08	0.32	7	11	0.44
HadRT2.0_500	-0.01	0.08	**0.10**	0.04	**-2.83**	1.35	0.23	7	11	0.48
HadRT2.0_300	0.03	0.10	**0.13**	0.05	**-3.19**	1.71	0.17	7	11	0.49
HadRT2.0_200	**-0.16**	0.13	**0.10**	0.06	**-3.34**	2.21	0.09	7	11	0.55
HadRT2.1_150	**-0.33**	0.15	**0.14**	0.06	**-4.07**	2.48	0.17	7	11	0.63
HadRT2.1_100	**-0.50**	0.10	**0.17**	0.05	**5.46**	1.71	0.54	4	0	0.43
HadRT2.1_50	**-0.92**	0.19	-0.08	0.09	**16.06**	3.34	0.50	6	0	0.62
Tropics										
JONES	**0.19**	0.08	**0.15**	0.04	**-1.96**	1.37	0.48	4	0	0.58
MOHSST	0.13	0.21	0.01	0.02	0.00	1.81	0.04	2	0	0.94
MOHSST (ols)	**0.15**	0.02	**0.06**	0.01	**-1.20**	0.31	0.89	4	7	0.00
NMAT	0.07	0.14	**0.05**	0.02	0.04	1.64	0.14	2	1	0.89
MSU 2lt	-0.02	0.20	**0.06**	0.04	-0.86	2.72	0.03	4	7	0.86
MSU 2	0.08	0.16	**0.09**	0.05	-2.23	2.49	0.07	4	9	0.81
MSU 4	**-0.31**	0.29	**-0.15**	0.12	**13.50**	4.98	0.13	0	0	0.66
HadRT2.0_850	**-0.07**	0.05	**0.11**	0.03	**-1.66**	0.82	0.47	4	10	0.26
HadRT2.0_700	**-0.12**	0.08	**0.18**	0.04	**-2.67**	1.37	0.38	4	10	0.43
HadRT2.0_500	**-0.11**	0.09	**0.15**	0.05	**-2.60**	1.61	0.22	4	10	0.48
HadRT2.0_300	-0.03	0.13	**0.21**	0.07	**-3.13**	2.29	0.20	4	10	0.52
HadRT2.0_200	**-0.15**	0.13	**0.27**	0.07	**-4.31**	2.31	0.24	4	10	0.50
HadRT2.1_150	**-0.31**	0.12	**0.25**	0.06	**-3.95**	2.06	0.28	4	10	0.40
HadRT2.1_100	**-0.39**	0.17	**0.24**	0.09	2.94	2.97	0.27	4	0	0.38
HadRT2.1_50	**-1.09**	0.50	-0.13	0.19	**22.62**	8.37	0.21	5	0	0.71
N. Hemi										
JONES	**0.32**	0.14	**0.10**	0.08	**-4.12**	2.51	0.30	9	8	0.45
MOHSST	**0.25**	0.08	0.03	0.03	**-1.89**	1.35	0.27	10	10	0.77
NMAT	**0.24**	0.11	0.02	0.05	**-2.01**	1.84	0.24	10	11	0.59
MSU 2lt	**0.16**	0.08	**0.10**	0.04	**-4.99**	1.40	0.24	9	5	0.44
MSU 2	**0.07**	0.06	**0.11**	0.03	**-3.98**	1.11	0.25	8	6	0.38
MSU 4	**-0.67**	0.18	**0.14**	0.10	**4.70**	3.24	0.24	3	0	0.47
HadRT2.0_850	**0.15**	0.11	**0.11**	0.06	**-4.66**	1.98	0.20	8	7	0.36
HadRT2.0_700	**0.10**	0.09	**0.12**	0.05	**-4.42**	1.59	0.28	8	7	0.36
HadRT2.0_500	0.09	0.09	**0.12**	0.05	**-4.50**	1.56	0.30	8	7	0.33
HadRT2.0_300	0.05	0.11	**0.11**	0.06	**-4.72**	1.98	0.16	8	7	0.38
HadRT2.0_200	-0.17	0.21	0.09	0.10	**-4.43**	3.71	0.04	8	7	0.56
HadRT2.1_150	**-0.34**	0.20	**0.14**	0.10	**-3.66**	3.53	0.09	8	7	0.57
HadRT2.1_100	**-0.52**	0.18	**0.18**	0.09	-2.51	3.08	0.20	2	11	0.49
HadRT2.1_50	**-0.90**	0.28	-0.06	0.13	**8.61**	4.91	0.23	5	0	0.62
S. Hemi										
JONES	0.03	0.09	-0.02	0.05	**-2.57**	1.58	0.17	0	2	0.27
MOHSST	**0.06**	0.05	0.02	0.03	-0.77	0.88	0.51	7	4	0.32
NMAT	**-0.17**	0.08	**-0.04**	0.04	0.29	1.42	0.37	0	4	0.46
MSU 2lt	-0.02	0.06	**0.07**	0.03	**-2.83**	1.02	0.14	8	10	0.32
MSU 2	**-0.08**	0.06	**0.06**	0.03	**-1.97**	1.12	0.10	8	11	0.42
MSU 4	**-0.54**	0.32	**-0.15**	0.12	**12.05**	5.36	0.13	3	0	0.74
HadRT2.0_850	-0.04	0.09	**0.03**	0.05	**-2.44**	1.58	0.07	8	11	0.22
HadRT2.0_700	-0.04	0.09	**0.06**	0.05	**-1.89**	1.68	0.07	8	11	0.24
HadRT2.0_500	0.00	0.12	**0.08**	0.07	**-2.41**	2.15	0.05	8	11	0.31
HadRT2.0_300	0.06	0.14	**0.10**	0.08	**-2.91**	2.53	0.05	8	11	0.38
HadRT2.0_200	-0.17	0.24	-0.02	0.12	-1.52	4.14	0.04	8	11	0.53
HadRT2.1_150	**-0.33**	0.27	-0.02	0.12	-2.38	4.63	0.05	8	11	0.60
HadRT2.1_100	**-0.60**	0.21	**0.15**	0.11	**11.09**	3.71	0.30	5	0	0.39
HadRT2.1_50	**-0.72**	0.29	**-0.15**	0.15	**18.23**	5.18	0.28	0	0	0.49

Table 1. Fits of monthly temperature series, 1979-1998, using REML regression except where indicated (OLS), to estimate, simultaneously, intercept, linear trend (°C/decade) and the effects of ENSO (°C/°C Nino3 anomaly) and volcanic eruptions (°C/optical depth @ 0.55μm). Boldface indicates a value significantly different from zero at the 95% level of confidence: 2σ error bars are also given. The fractional variances explained by the fits are given in the r^2 column. The temperature series were lagged behind ENSO and the volcanic eruptions so as to optimise the fits (see text) by the interval, in months, given in the "ENSO shift" and "Vol shift" columns. The serial correlations of the original series are given in the final column.

Global	Trend	err	ENSO	err	Volcano	err	r^2	ENSO shift	Vol shift	Serial corr
JONES/MOHSST - NMAT	**0.12**	0.04	**0.03**	0.02	-0.70	0.76	0.14	8	7	0.29
JONES/MOHSST - MSU 2lt	**0.14**	0.04	**-0.06**	0.02	**2.16**	0.78	0.62	6	4	0.41
JONES/MOHSST - MSU 2	**0.16**	0.04	**-0.06**	0.02	**1.26**	0.76	0.62	6	11	0.36
JONES/MOHSST - MSU 4	**0.68**	0.12	0.03	0.04	**-10.20**	1.91	0.53	6	0	0.73
JONES/MOHSST - HadRT2.0_850	**0.13**	0.04	**0.04**	0.02	**1.13**	0.76	0.33	0	11	0.28
JONES/MOHSST - HadRT2.0_700	**0.19**	0.05	**-0.05**	0.03	**1.28**	0.95	0.26	7	11	0.33
JONES/MOHSST - HadRT2.0_500	**0.18**	0.07	**-0.06**	0.04	**1.42**	1.21	0.20	7	11	0.38
JONES/MOHSST - HadRT2.0_300	**0.15**	0.09	**-0.09**	0.05	**1.78**	1.61	0.15	7	11	0.41
JONES/MOHSST - HadRT2.0_200	**0.34**	0.13	-0.06	0.07	1.93	2.27	0.27	7	11	0.52
JONES/MOHSST - HadRT2.1_150	**0.51**	0.15	**-0.10**	0.07	**2.72**	2.55	0.33	7	11	0.61
JONES/MOHSST - HadRT2.1_100	**0.67**	0.09	**-0.12**	0.05	**-6.48**	1.60	0.73	4	0	0.37
JONES/MOHSST - HadRT2.1_50	**1.09**	0.17	**0.11**	0.08	**-17.00**	2.96	0.66	6	0	0.55
Tropics										
JONES/MOHSST - NMAT	**0.09**	0.02	**0.01**	0.01	-0.17	0.34	0.33	5	11	0.28
JONES/MOHSST - MSU 2lt	**0.19**	0.05	**-0.07**	0.02	**2.26**	0.80	0.64	7	9	0.41
JONES/MOHSST - MSU 2	**0.12**	0.05	**-0.09**	0.03	**1.71**	0.83	0.59	7	11	0.35
JONES/MOHSST - MSU 4	**0.49**	0.29	**0.16**	0.13	**-13.45**	5.06	0.16	1	0	0.65
JONES/MOHSST - HadRT2.0_850	**0.21**	0.04	**0.08**	0.02	0.41	0.68	0.51	0	11	0.19
JONES/MOHSST - HadRT2.0_700	**0.28**	0.06	**-0.05**	0.03	**1.33**	1.10	0.28	6	11	0.33
JONES/MOHSST - HadRT2.0_500	**0.28**	0.07	**-0.06**	0.04	**1.36**	1.22	0.30	6	11	0.33
JONES/MOHSST - HadRT2.0_300	**0.20**	0.10	**-0.13**	0.05	**2.19**	1.68	0.17	6	11	0.37
JONES/MOHSST - HadRT2.0_200	**0.30**	0.12	**-0.12**	0.06	**3.23**	2.01	0.23	6	11	0.43
JONES/MOHSST - HadRT2.1_150	**0.47**	0.11	**-0.11**	0.06	**3.02**	1.98	0.41	6	11	0.38
JONES/MOHSST - HadRT2.1_100	**0.54**	0.17	**-0.10**	0.09	**-4.50**	3.02	0.39	8	0	0.38
JONES/MOHSST - HadRT2.1_50	**1.25**	0.50	**0.20**	0.20	**-23.24**	8.48	0.26	5	0	0.70
N. Hemi										
JONES/MOHSST - NMAT	0.04	0.12	0.06	0.07	-1.33	2.26	0.02	11	8	0.41
JONES/MOHSST - MSU 2lt	**0.13**	0.08	**-0.06**	0.04	**3.02**	1.39	0.41	6	2	0.42
JONES/MOHSST - MSU 2	**0.22**	0.10	**-0.08**	0.05	**1.81**	1.75	0.32	5	3	0.49
JONES/MOHSST - MSU 4	**0.95**	0.24	-0.11	0.12	**-6.20**	4.35	0.24	3	0	0.56
JONES/MOHSST - HadRT2.0_850	**0.13**	0.07	**-0.06**	0.04	**1.87**	1.30	0.17	7	5	0.26
JONES/MOHSST - HadRT2.0_700	**0.18**	0.08	**-0.06**	0.04	**1.83**	1.40	0.16	7	5	0.30
JONES/MOHSST - HadRT2.0_500	**0.19**	0.09	**-0.07**	0.05	**2.30**	1.61	0.13	7	5	0.29
JONES/MOHSST - HadRT2.0_300	**0.24**	0.14	**-0.09**	0.08	**3.14**	2.56	0.11	7	5	0.44
JONES/MOHSST - HadRT2.0_200	**0.47**	0.26	-0.08	0.12	2.56	4.54	0.13	7	5	0.61
JONES/MOHSST - HadRT2.1_150	**0.65**	0.27	**-0.14**	0.12	1.29	4.72	0.16	7	5	0.65
JONES/MOHSST - HadRT2.1_100	**0.81**	0.24	**-0.12**	0.12	**-4.48**	4.20	0.29	2	0	0.57
JONES/MOHSST - HadRT2.1_50	**1.18**	0.31	0.11	0.14	**-9.90**	5.27	0.34	9	0	0.61
S. Hemi										
JONES/MOHSST - NMAT	**0.24**	0.09	0.04	0.05	-1.03	1.65	0.14	0	4	0.41
JONES/MOHSST - MSU 2lt	**0.08**	0.06	**-0.06**	0.04	**2.32**	1.10	0.36	8	11	0.27
JONES/MOHSST - MSU 2	**0.15**	0.07	**-0.06**	0.04	**1.57**	1.28	0.30	9	11	0.32
JONES/MOHSST - MSU 4	**0.60**	0.29	0.07	0.12	**-11.91**	4.93	0.15	7	0	0.66
JONES/MOHSST - HadRT2.0_850	**0.11**	0.07	**-0.05**	0.04	**2.17**	1.32	0.18	9	11	0.09
JONES/MOHSST - HadRT2.0_700	**0.11**	0.09	**-0.07**	0.05	1.53	1.57	0.11	9	11	0.12
JONES/MOHSST - HadRT2.0_500	0.06	0.12	**-0.08**	0.07	2.02	2.08	0.07	9	11	0.22
JONES/MOHSST - HadRT2.0_300	0.00	0.14	**-0.10**	0.08	**2.54**	2.54	0.08	9	11	0.30
JONES/MOHSST - HadRT2.0_200	**0.25**	0.24	-0.02	0.12	1.46	4.22	0.11	9	11	0.50
JONES/MOHSST - HadRT2.1_150	**0.42**	0.27	-0.04	0.13	2.55	4.79	0.11	9	11	0.59
JONES/MOHSST - HadRT2.1_100	**0.66**	0.22	**-0.15**	0.12	**-11.68**	3.87	0.36	4	0	0.40
JONES/MOHSST - HadRT2.1_50	**0.79**	0.28	**0.15**	0.15	**-18.79**	5.11	0.35	0	0	0.48

Table 2. As Table 1, but for differences, i.e. JONES/MOHSST minus temperature series.

Tropics	Trend	err	ENSO	err	Volcano	err	r^2	ENSO shift	Vol shift	Serial corr
HadRT2.0_850 - HadRT2.0_700	0.01	0.06	**-0.09**	0.04	0.54	1.09	0.11	3	10	0.38
HadRT2.0_850 - HadRT2.0_500	0.05	0.07	**-0.08**	0.04	**1.34**	1.26	0.07	2	2	0.34
HadRT2.0_850 - HadRT2.0_300	0.07	0.10	**-0.14**	0.06	**3.23**	1.87	0.12	2	2	0.43
HadRT2.0_850 - HadRT2.0_200	**0.13**	0.13	**-0.15**	0.07	**2.78**	2.28	0.13	2	3	0.52
HadRT2.0_850 - HadRT2.1_150	**0.22**	0.14	**-0.13**	0.07	**2.47**	2.42	0.23	2	11	0.51
HadRT2.0_850 - HadRT2.1_100	**0.31**	0.17	**-0.16**	0.10	**-5.47**	2.96	0.40	3	0	0.36
HadRT2.0_850 - HadRT2.1_50.	**1.02**	0.45	**0.29**	0.19	**-24.40**	7.58	0.40	6	0	0.68

Table 3. As Table 2 but for tropical atmospheric differences only, i.e. tropical 850hPa temperature series minus the tropical temperature series aloft. Units are as in Table 1.

Prescribed ENSO shift months	Prescribed Volcano shift months	Trend °C/decade	ENSO	Volcano
0	0	**0.18**	-0.004	1.099
0	4	**0.18**	-0.004	**1.26**
0	8	**0.17**	-0.001	**1.433**
0	12	**0.17**	0.003	**1.675**
4	0	**0.19**	**-0.051**	**1.523**
4	4	**0.19**	**-0.056**	**1.767**
4	8	**0.19**	**-0.054**	**1.854**
4	12	**0.18**	**-0.043**	**1.778**
8	0	**0.19**	**-0.045**	**1.341**
8	4	**0.19**	**-0.054**	**1.722**
8	8	**0.19**	**-0.06**	**2.019**
8	12	**0.19**	**-0.056**	**2.085**
12	0	**0.17**	0.019	0.999
12	4	**0.17**	0.015	1.128
12	8	**0.17**	0.01	**1.336**
12	12	**0.17**	0.006	**1.61**

Table 4. Variation of the REML trend, ENSO and volcanic coefficients with varied shift times for ENSO and volcanoes, for 1979-1998 JONES/MOHSST minus MSU2LT tropical timeseries. Units are as in Table 1.

Regression	Trend (°C/decade)	ENSO	Volcano	VOT	VOF	SSE	r^2	MSE	serial cor
JONES/MOHSST ols	0.15	0.17	-1.70	24.15	21.51	2.64	0.89	0.011	0.00
JONES/MOHSST reml	0.15	0.02	0.39	1.55	0.12	1.44	0.08	0.006	0.92
MSUlt ols	-0.04	0.24	-3.80	20.44	13.50	6.93	0.66	0.029	0.00
MSUlt reml	-0.02	0.06	-0.86	4.47	0.15	4.32	0.03	0.018	0.86
JO/MO - MSUlt ols	0.20	-0.07	1.99	20.78	16.40	4.38	0.79	0.019	0.00
JO/MO - MSUlt reml	0.19	-0.06	1.78	8.43	4.81	3.62	0.57	0.015	0.45
JO/MO - MSUlt indep	0.20	-0.05	1.32	6.63	1.47	5.16	0.22	0.022	0.38
JO/MO - MSUlt grdp	0.19	-0.01	0.48	4.32	1.07	3.25	0.25	0.014	0.40

Table 5. Fits of monthly tropical temperature and temperature difference series, 1979-1998, using OLS and REML regression, to estimate, simultaneously, intercept, linear trend and the influences of ENSO and volcanic eruptions. VOT is variance of timeseries (once serial correlation has been removed if appropriate), VOF variance of fit, SSE sum of squared errors and MSE mean squared errors. “Indep” timeseries are where ENSO and volcanic influences are removed from surface and atmospheric temperatures prior to differencing. “Grdp” timeseries are where ENSO and volcanic influences are removed from individual grid points of surface minus tropospheric temperature differences prior to calculation of tropical avereage. Units are as in Table 1.

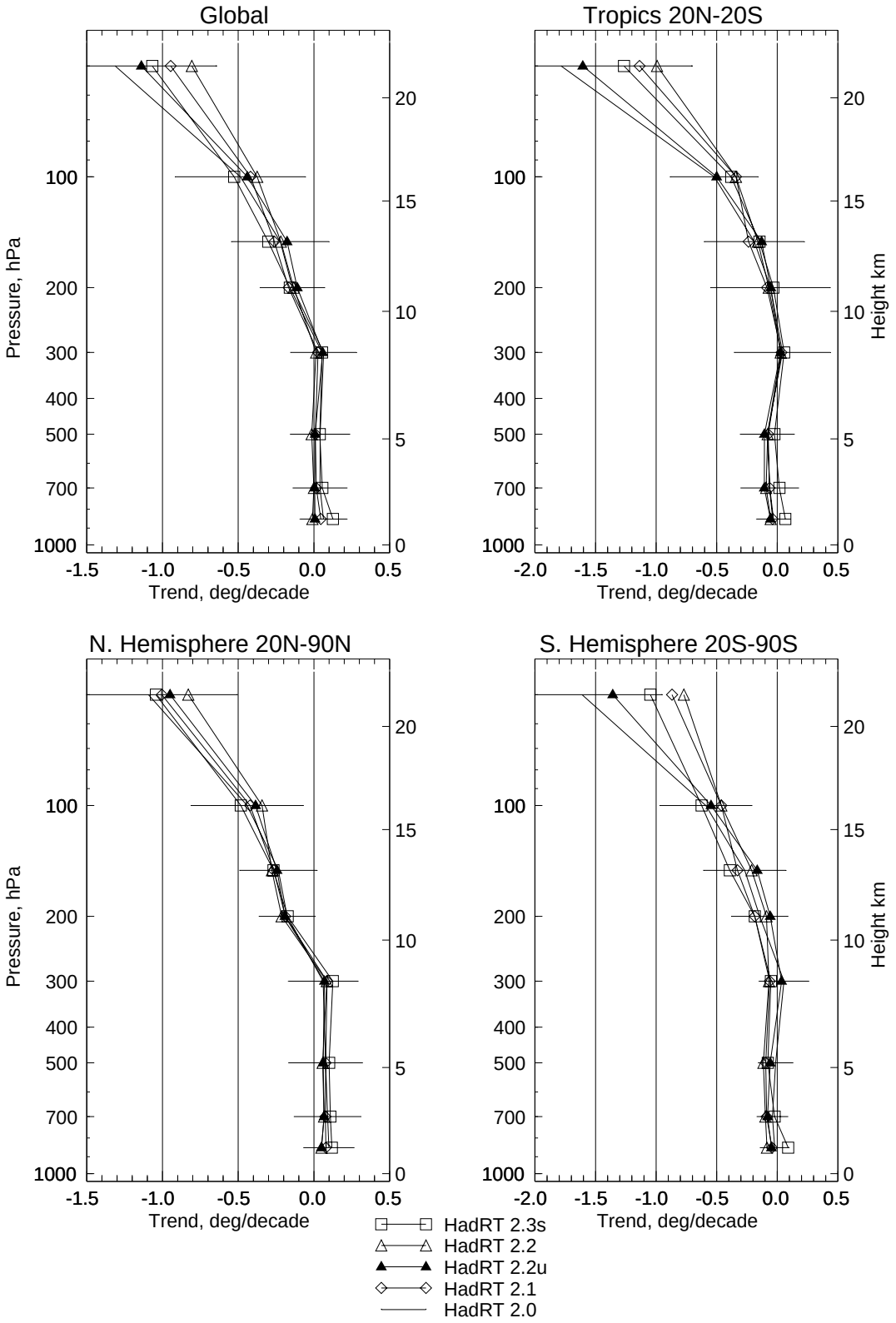

Figure 1a. Profiles of temperature trends calculated using REML with first-order autoregression term from seasonal temperature series for March-May 1979 through September-November 1998 based on all available data in the radiosonde-based HadRT datasets indicated.

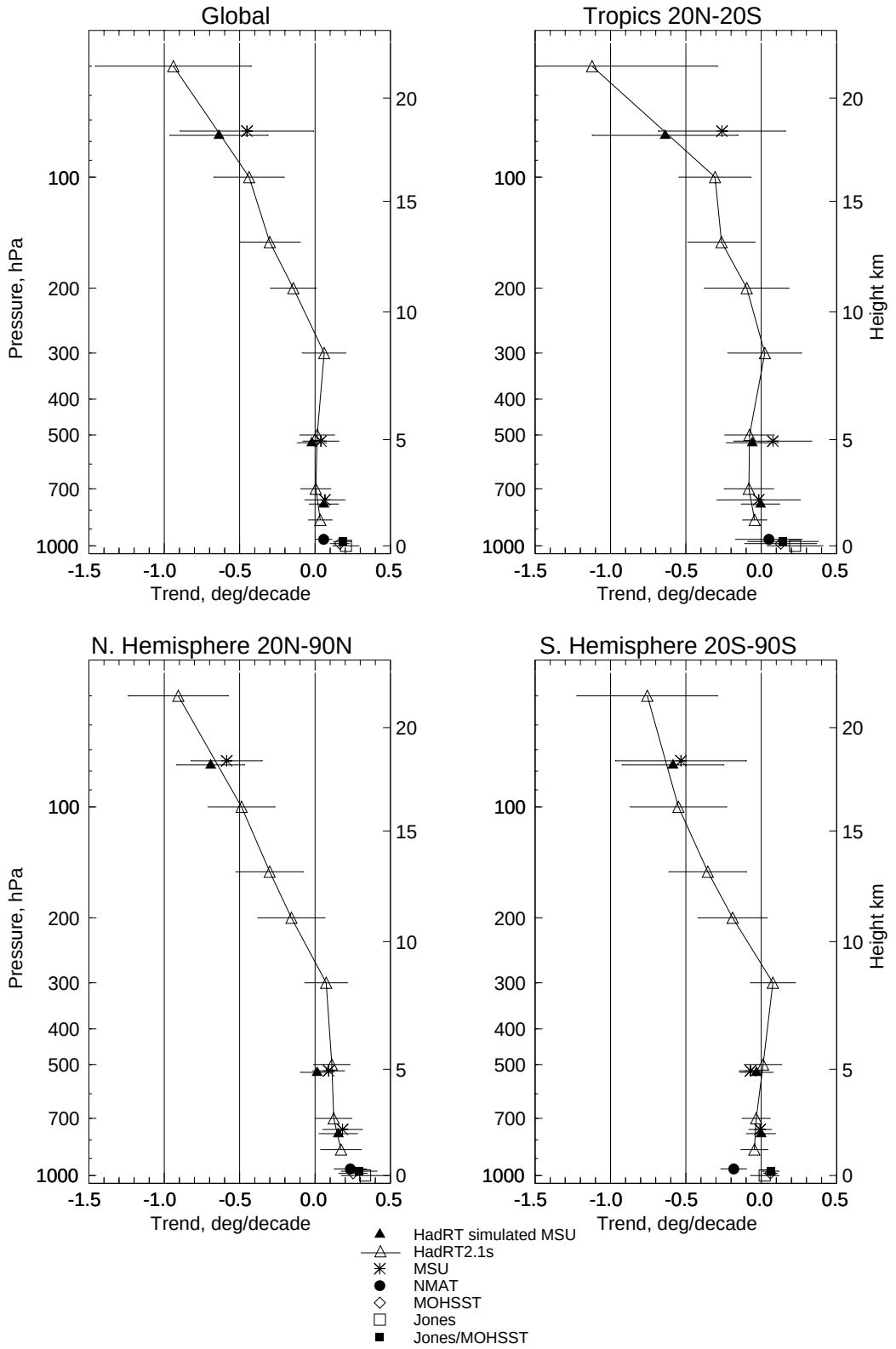

Figure 1b. Profiles of temperature trends calculated using REML with first-order autoregression term from monthly temperature series for 1979 to 1998 based on all available data in the HadRT, MSU and surface datasets indicated. MSU4, MSU2 and MSU2LT data are plotted at 75, 520 and 750 hPa respectively.

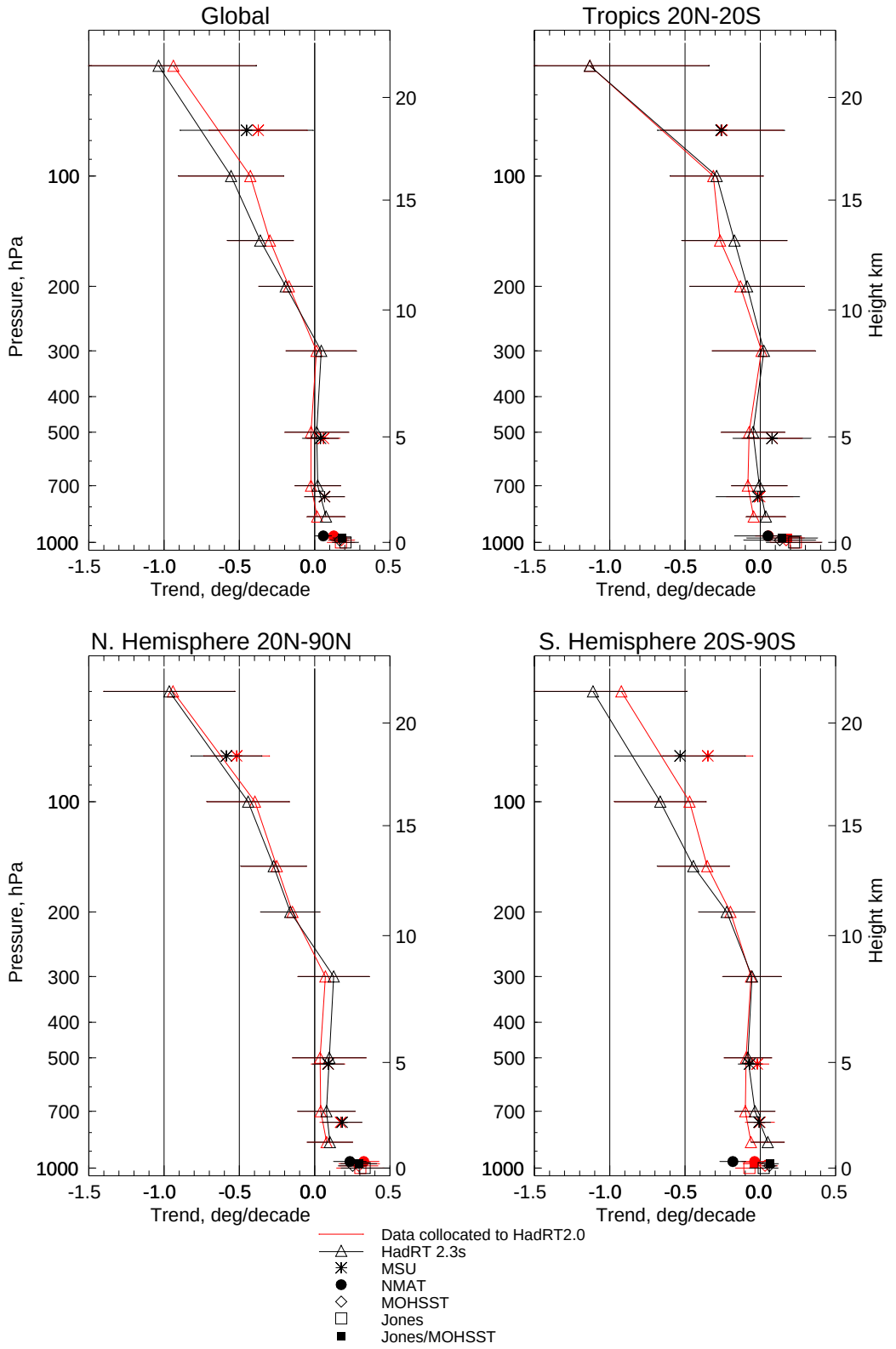

Figure 1c. Profiles of temperature trends calculated using REML with first-order autoregression term from monthly temperature series for 1979 to 1998 based on all available data in the spatially complete HadRT, MSU and surface datasets indicated (black) and on the same data but restricted to grid-boxes with data in the radiosonde-based data set HadRT2.0 (red).

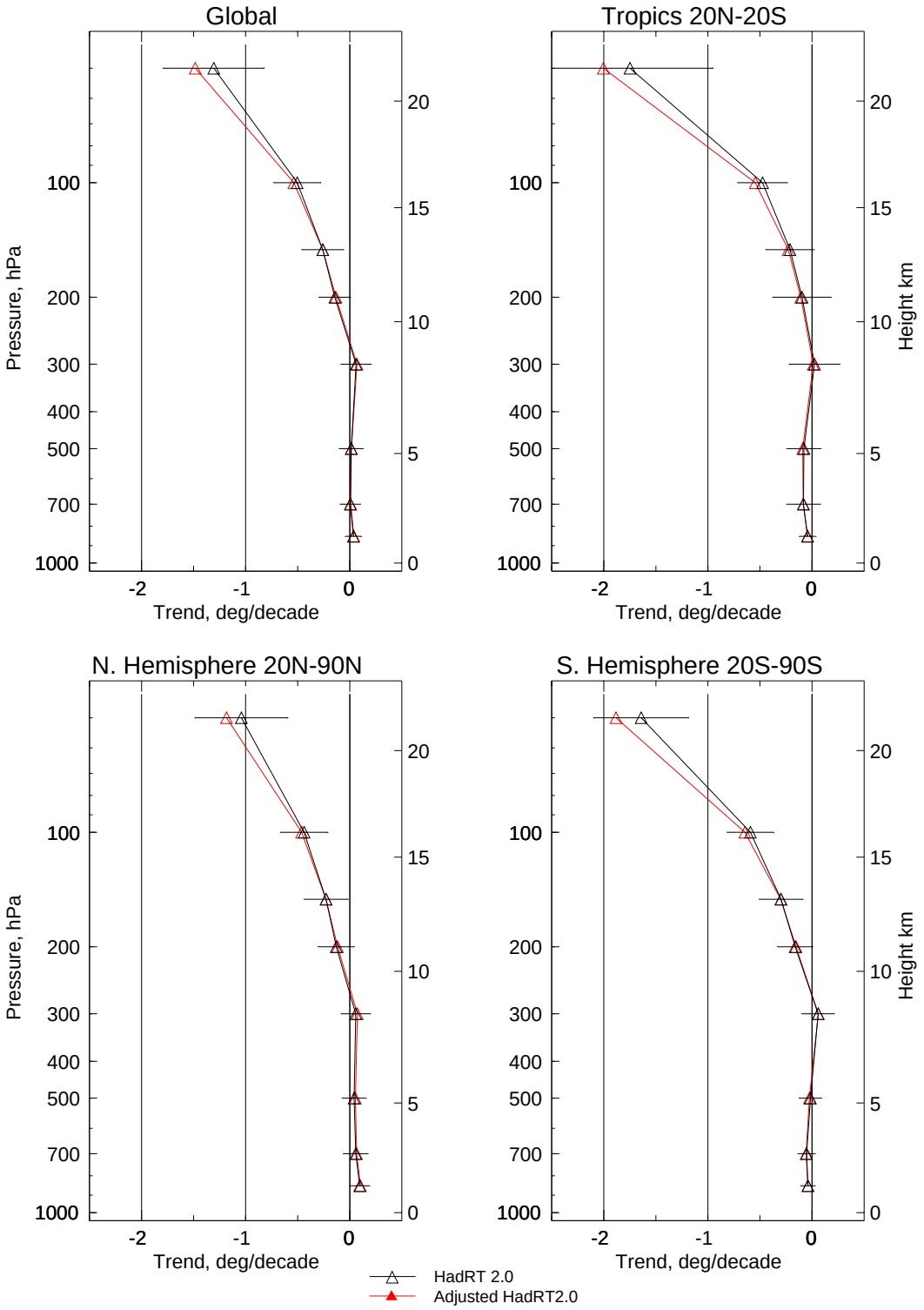

Figure 1d. Profiles of temperature trends calculated using REML with first-order autoregression term from monthly temperature series for 1979 to 1998 based on all available data in the radiosonde-based HadRT2.0 dataset. The black curves indicate trends at fixed pressure-levels, as shown in Figs. 1a to 1c: the red curves are adjusted to allow for changes in geopotential height arising from warming/cooling at lower levels, and thus effectively show trends at fixed height levels.

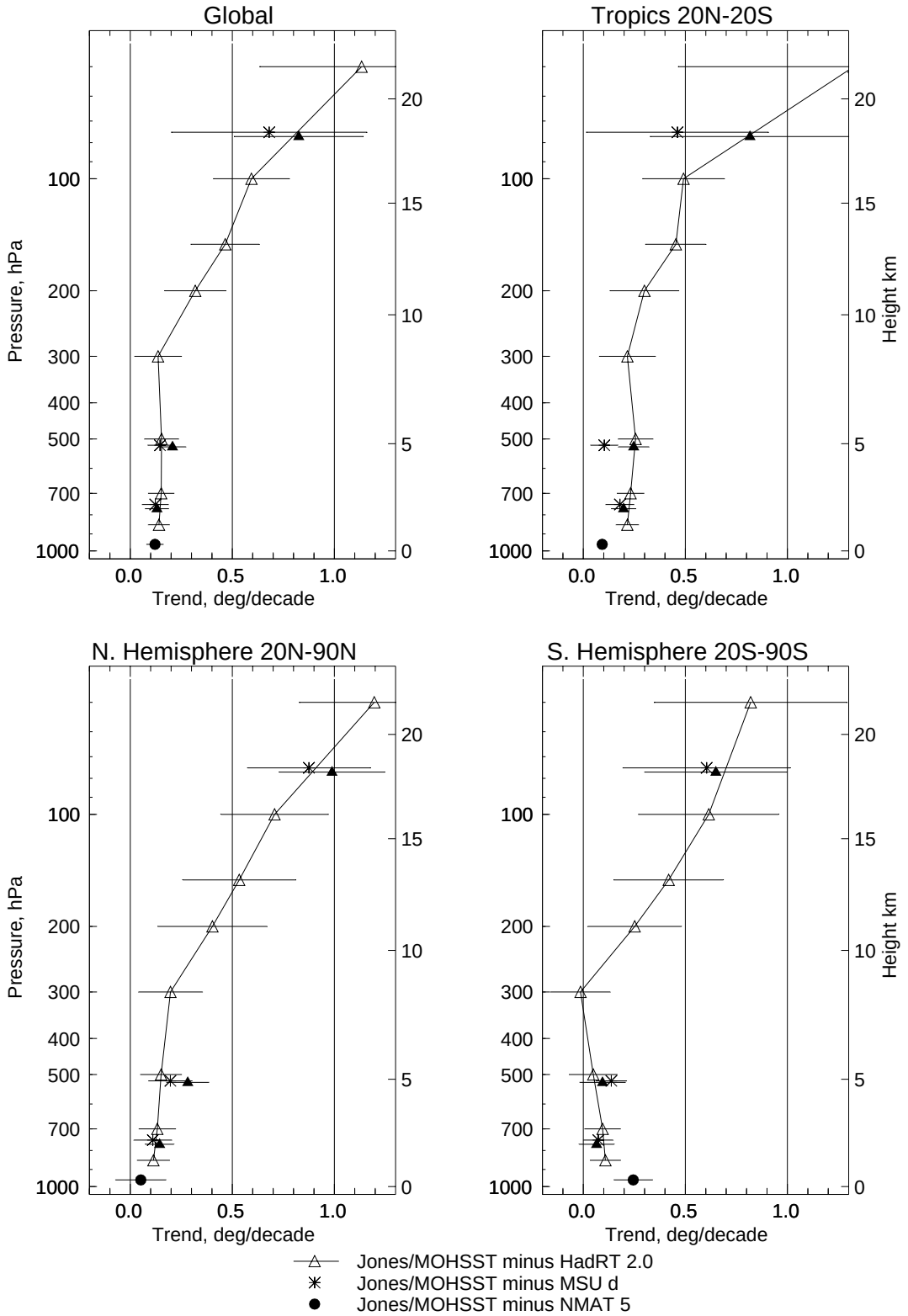

Figure 1e. Profiles of temperature trends calculated using REML with first-order autoregression term from monthly temperature difference series, JONES/MOHSST minus HadRT or MSU or NMAT, for 1979 to 1998 based on all available data in the respective datasets.

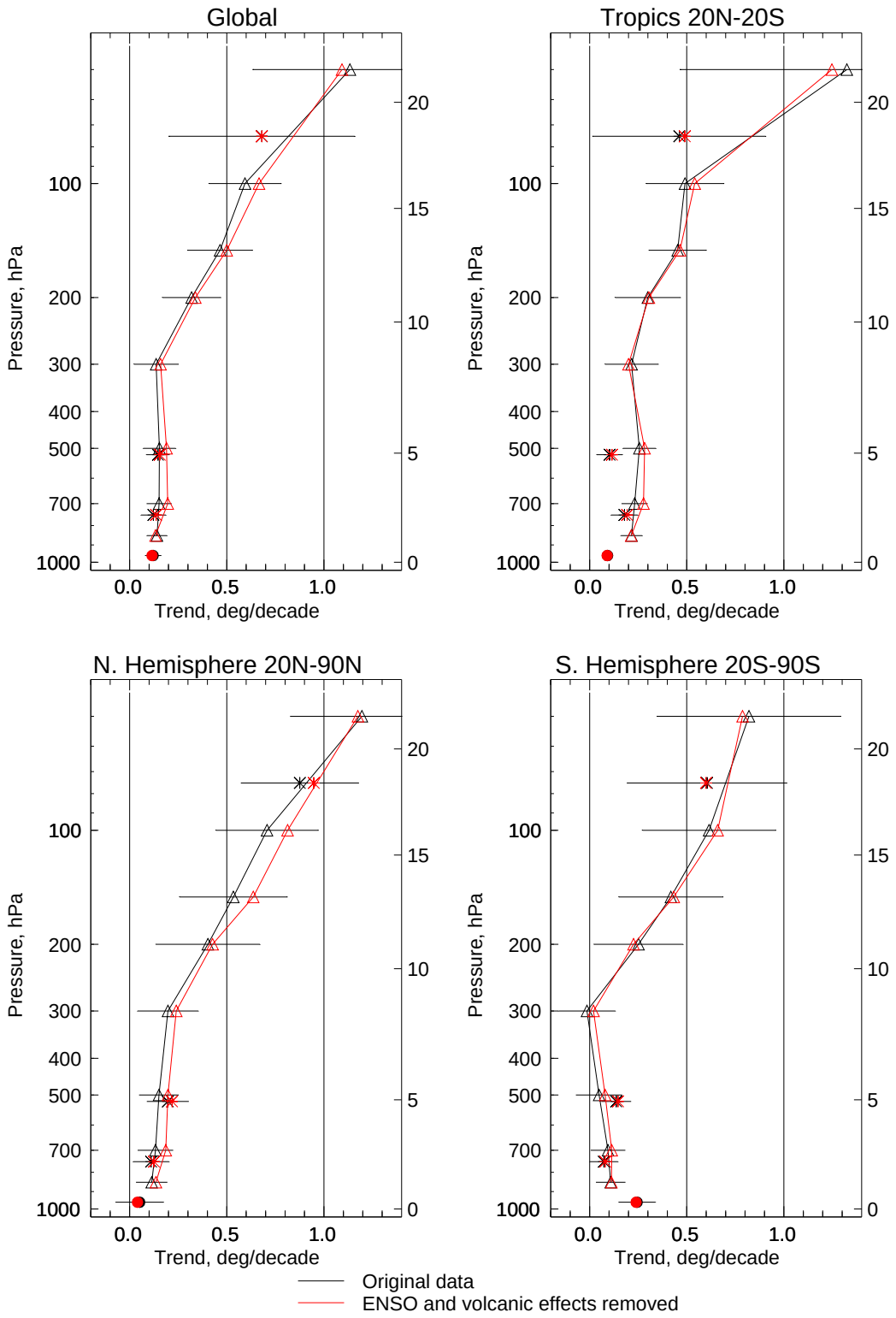

Figure 1f. Profiles of temperature trends calculated using REML with first-order autoregression term from monthly temperature difference series, JONES/MOHSST minus HadRT or MSU or NMAT, for 1979 to 1998 based on all available data in the respective datasets. The black lines and symbols are the same as in Fig. 1e; red items represent trends calculated after the removal of ENSO and volcanic influences.

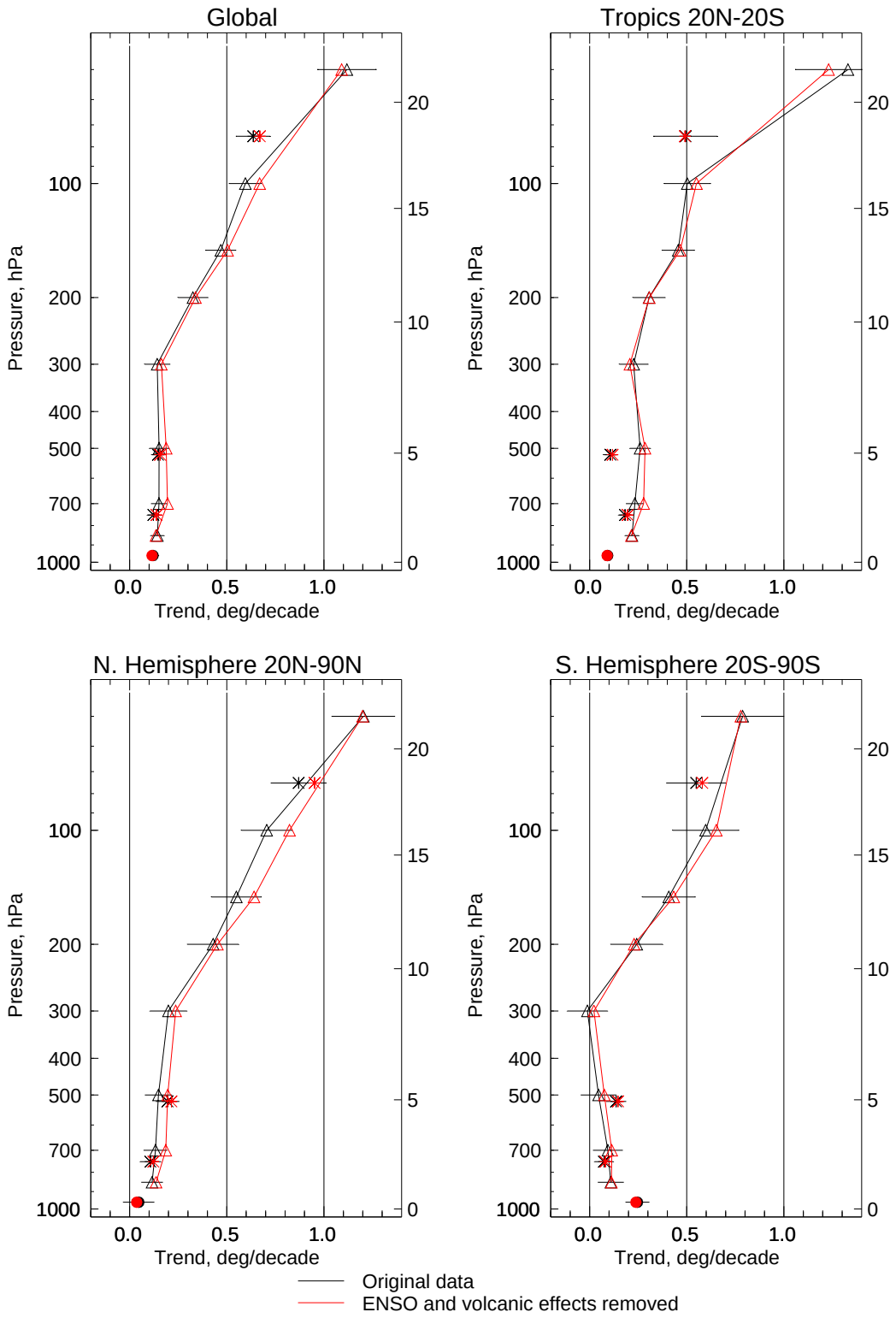

Figure 1g. As for figure 1f except using OLS (ordinary least squares)

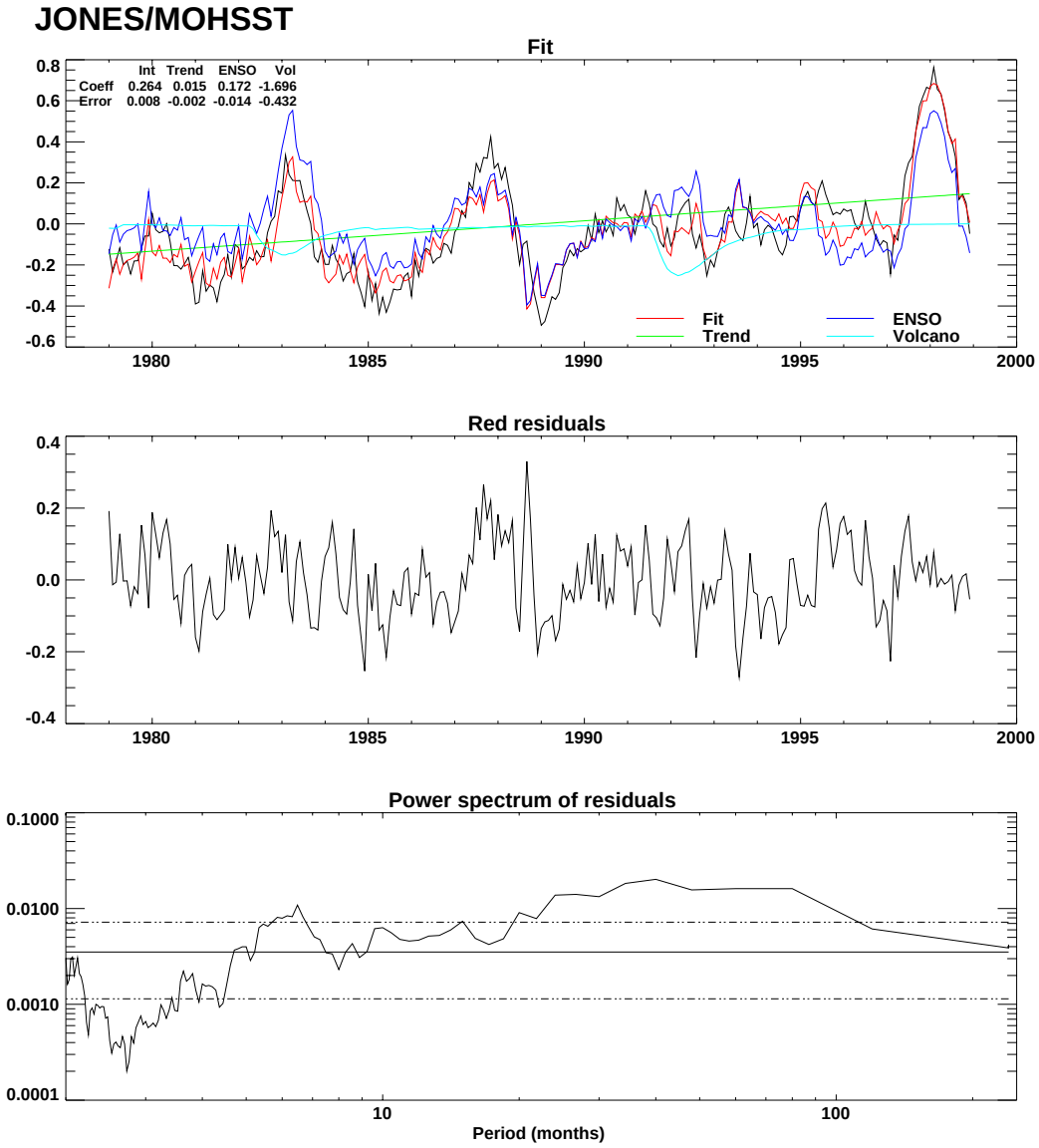

Figure 2a. Fit of monthly tropical JONES/MOHSST temperature series, 1979-1998, using OLS regression, to estimate, simultaneously, intercept, linear trend and the influences of ENSO and volcanic eruptions. The original series, the fitted trend, ENSO and volcanic components and the total fit are shown in the top panel. The second panel shows the residuals from the total fit and the bottom panel shows the power spectrum of these residuals.

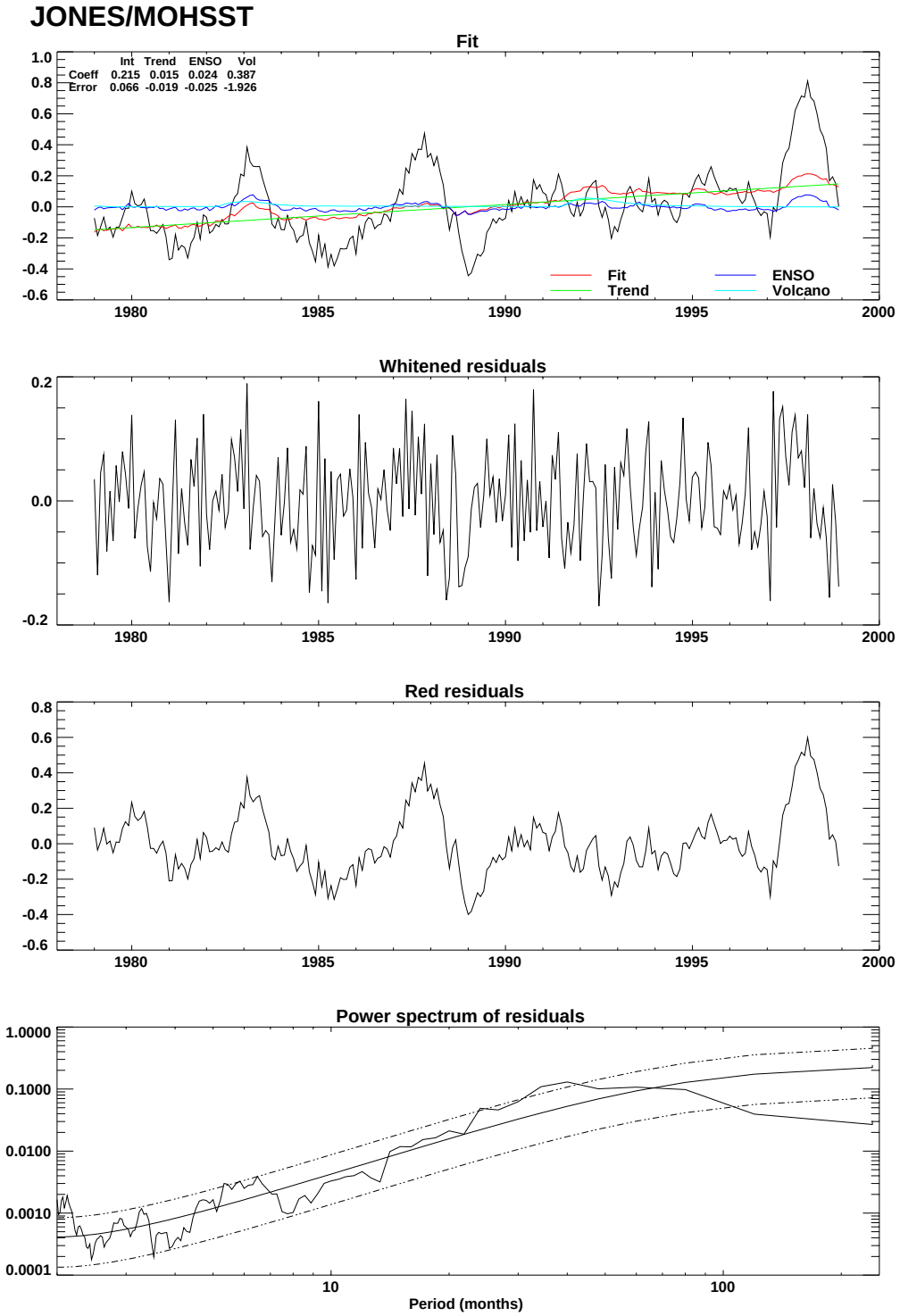

Figure 2b. Fit of monthly tropical JONES/MOHSST temperature series, 1979-1998, using REML regression with first order autoregression term, to estimate, simultaneously, intercept, linear trend and the influences of ENSO and volcanic eruptions. The original series, the fitted trend, ENSO and volcanic components and the total fit are shown in the top panel. The second panel shows the residuals after removal of the modelled autoregressive component. The third panel shows the residuals from the total fit. The bottom panel shows the power spectrum of residuals from the total fit.

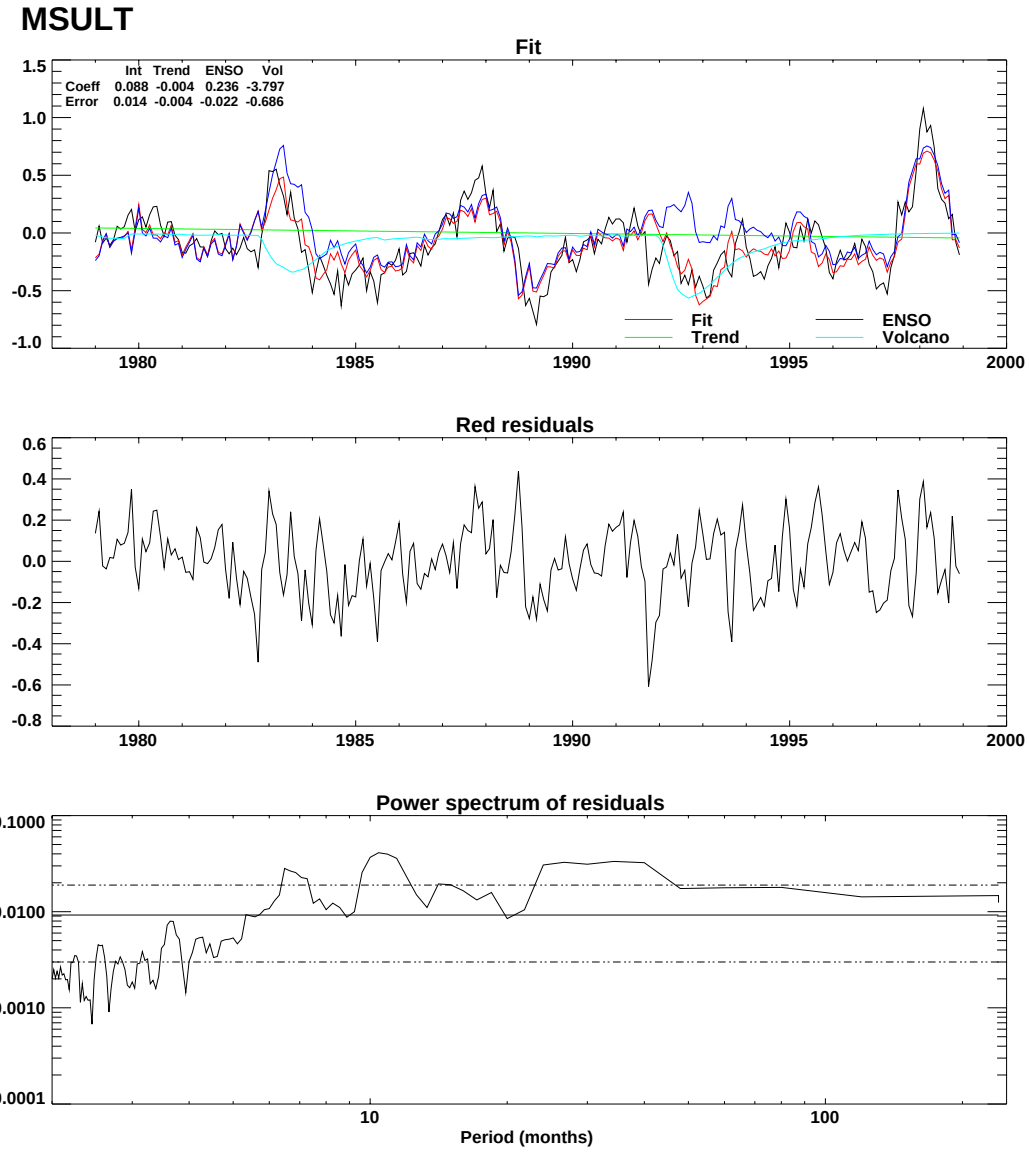

Figure 2c. As Fig. 2a, but for MSU2LT.

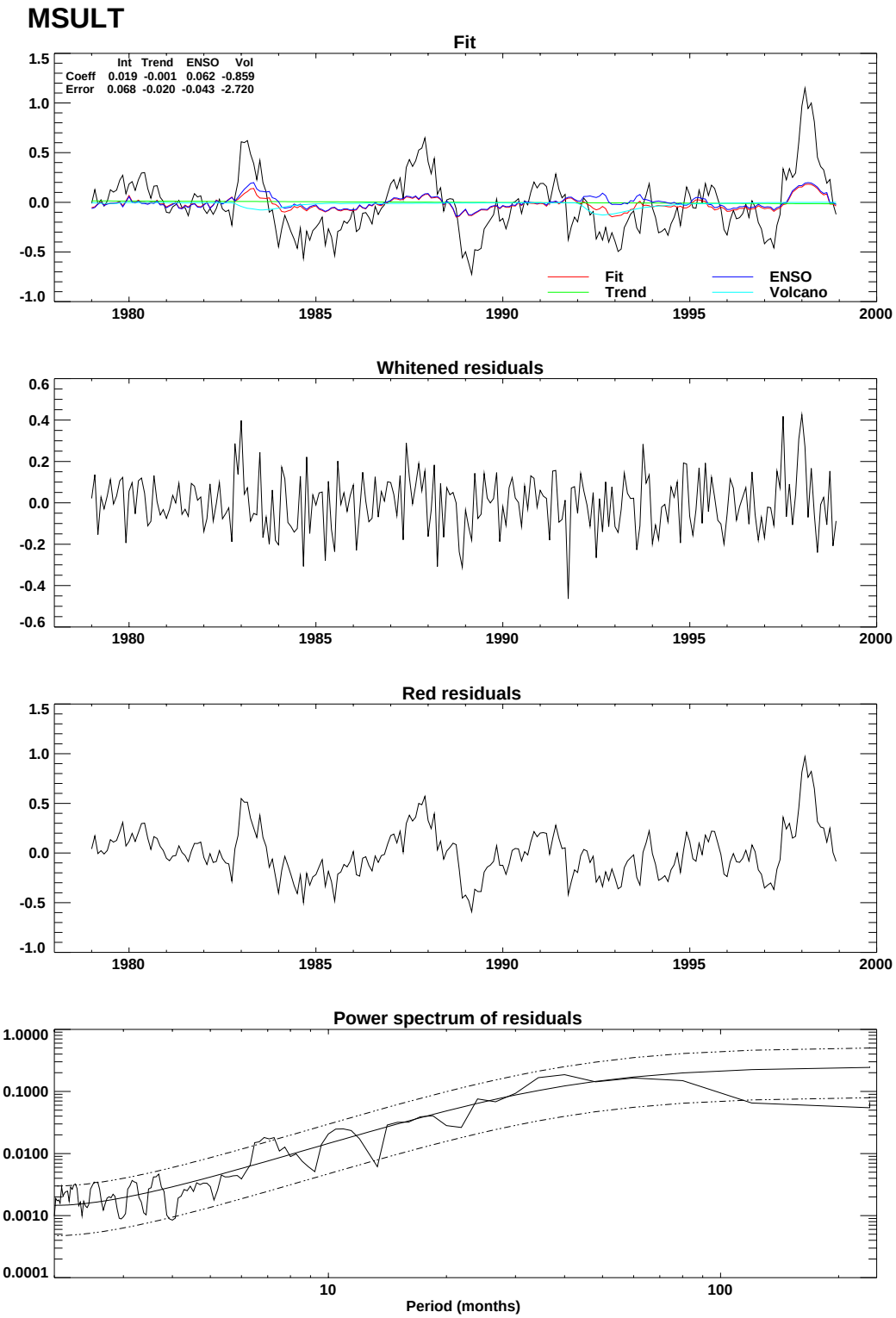

Figure 2d. As Fig. 2b, but for MSU2LT.

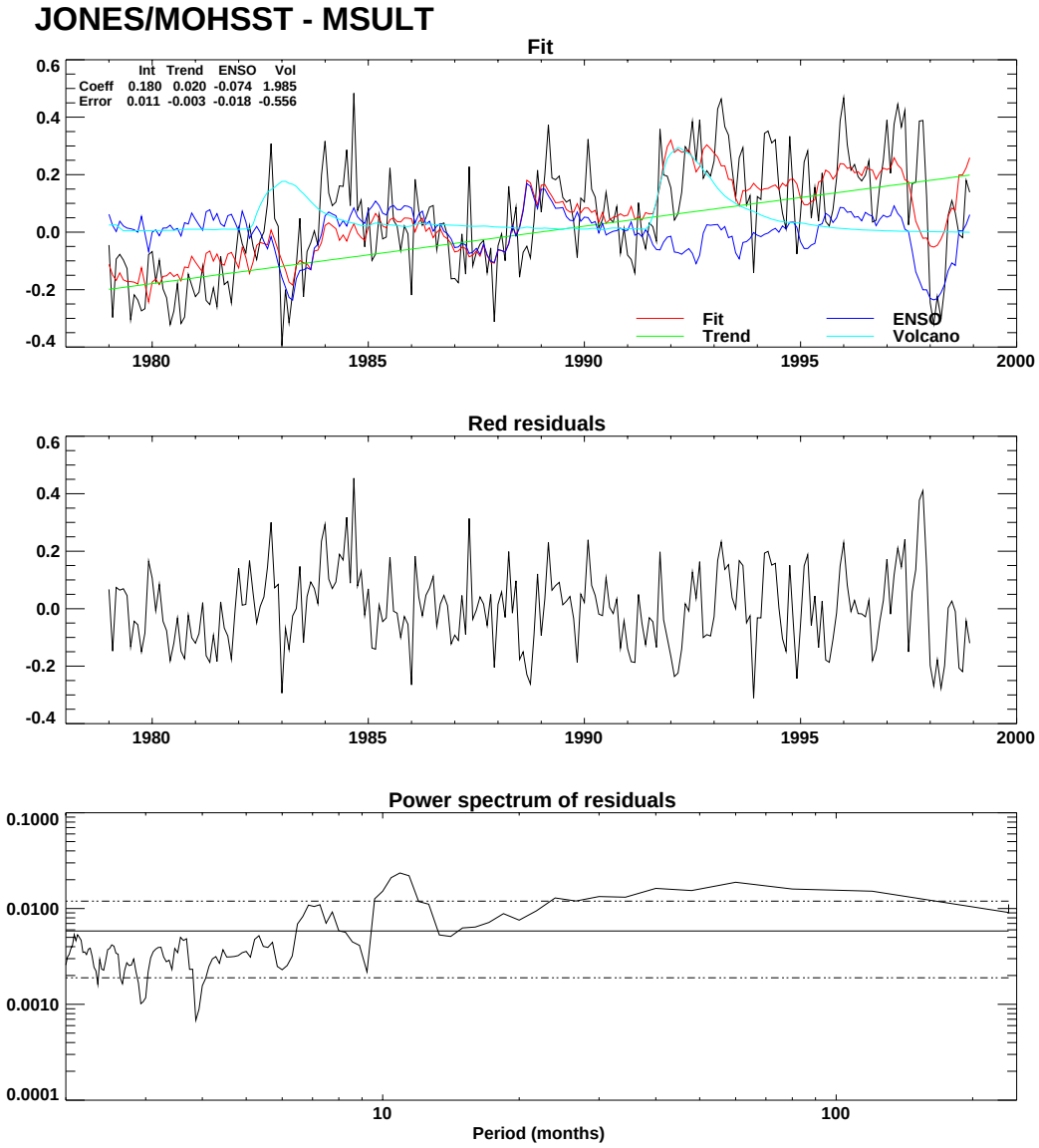

Figure 3a. As Fig. 2a, but for JONES/MOHSST minus MSU2LT.

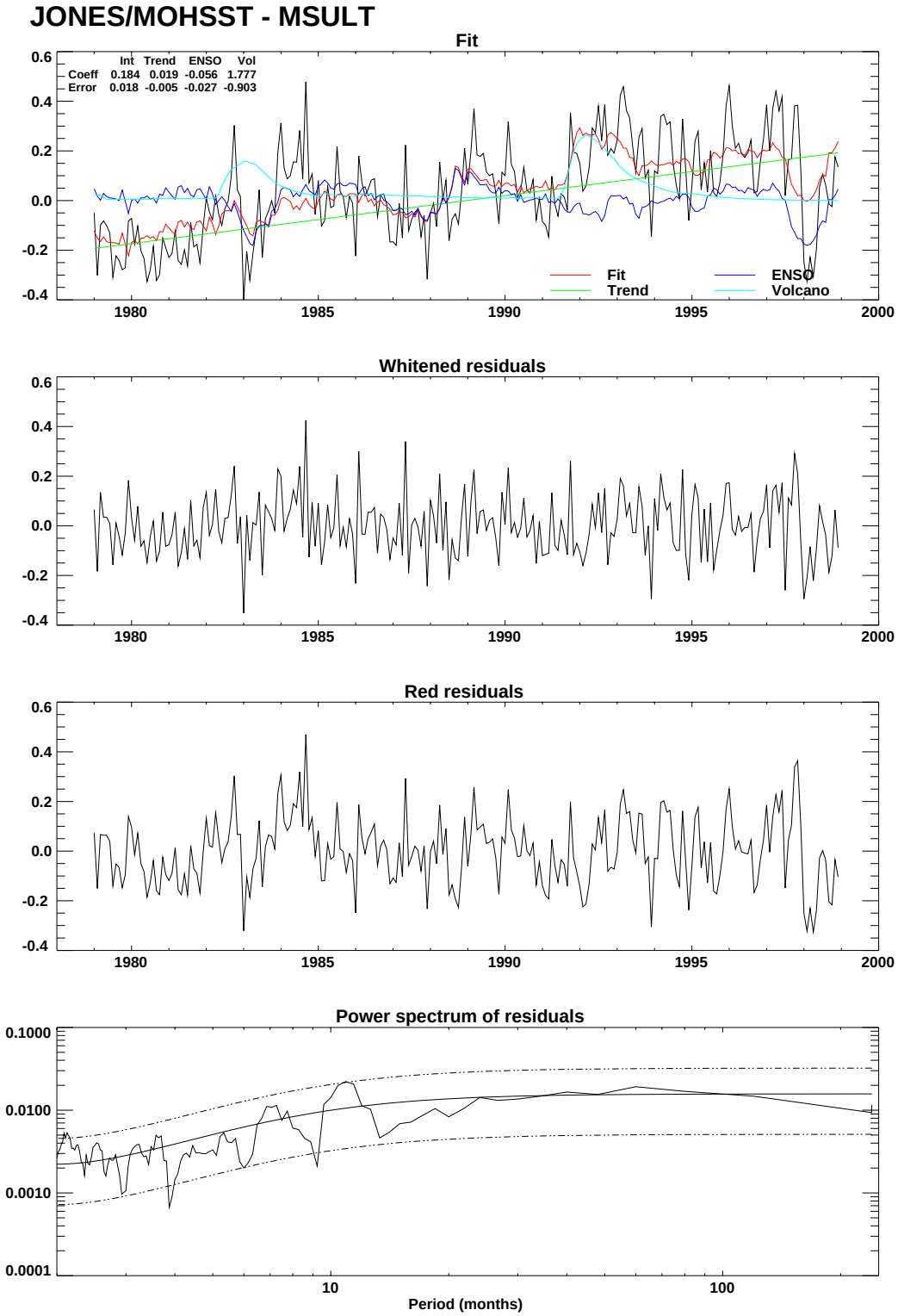

Figure 3b. As Fig. 2b, but for JONES/MOHSST minus MSU2LT.

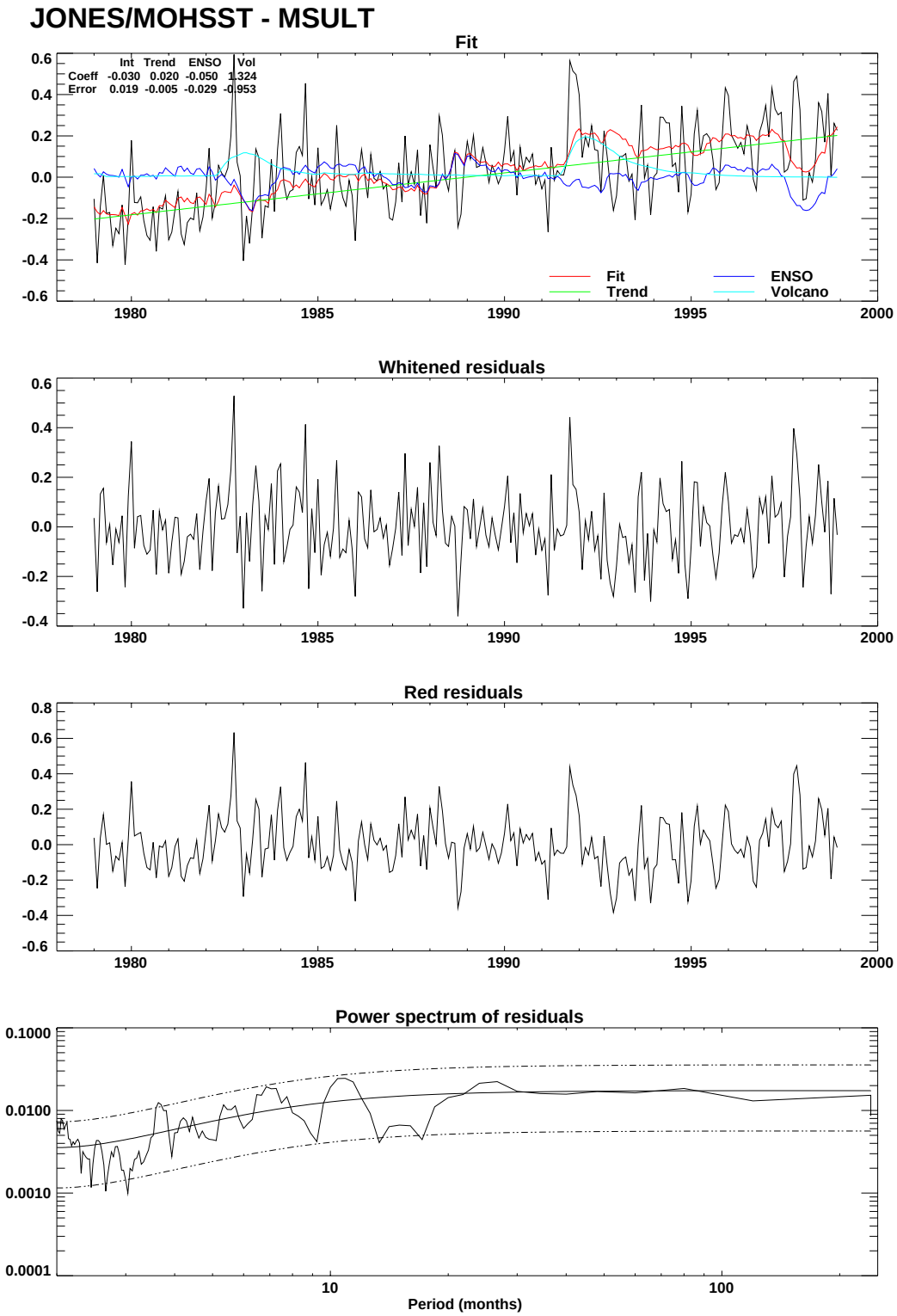

Figure 3c. As Fig 3b, but with ENSO and volcanic effects removed independently from the original series before differencing.

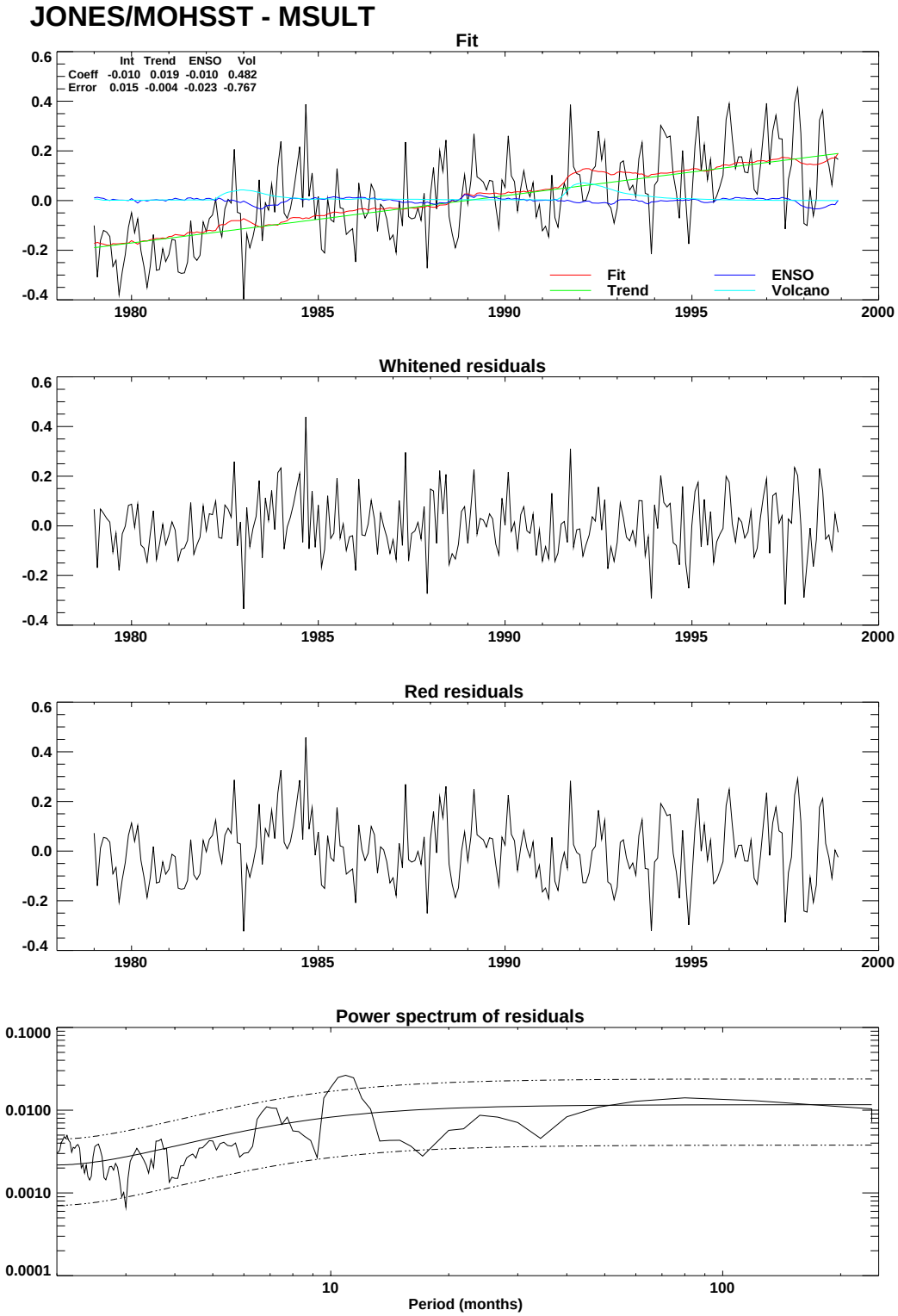

Figure 3d. As Fig. 3b, but with ENSO and volcanic effects removed independently from the original gridded data before differencing.

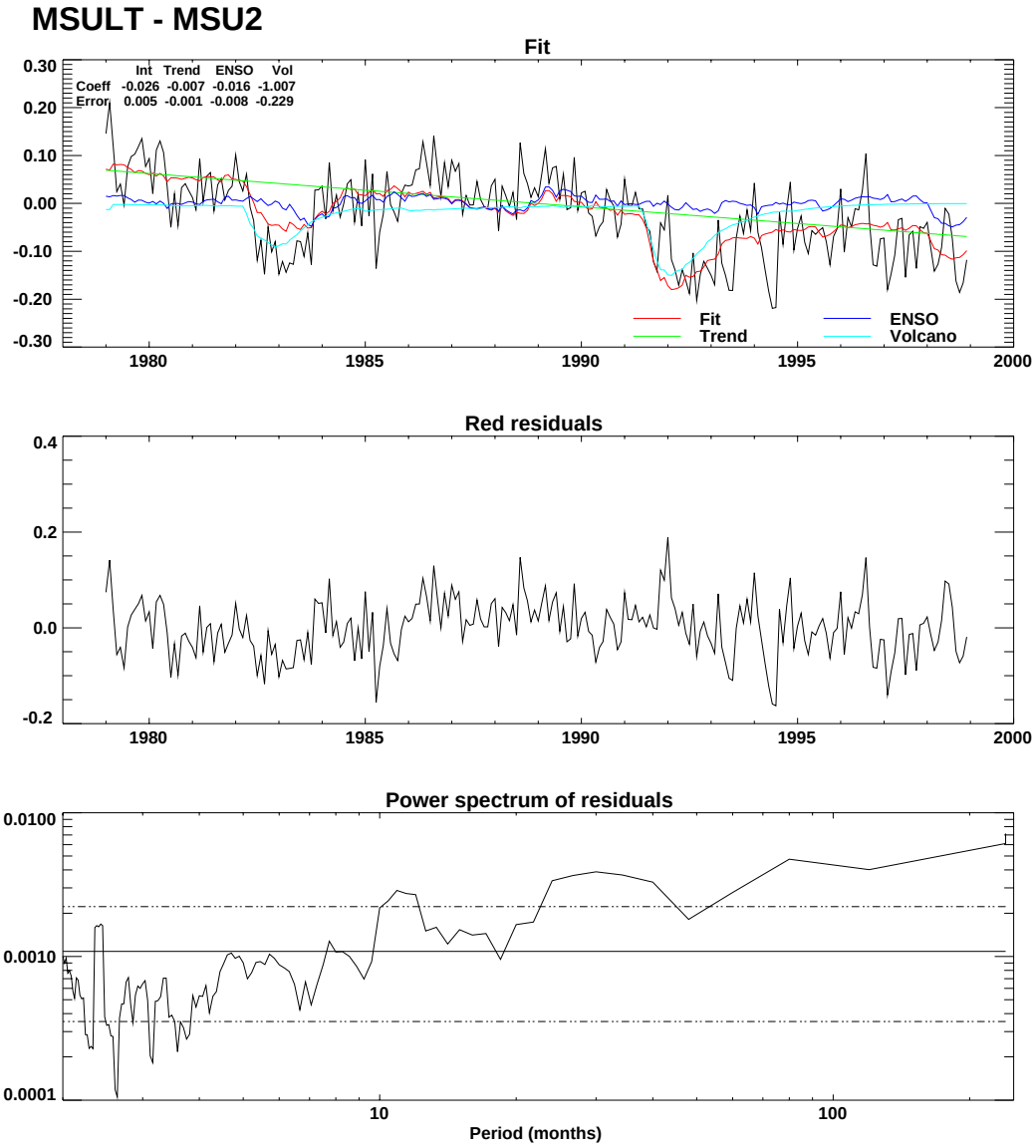

Figure 4a. As Fig. 2a, but for MSU2LT minus MSU2.

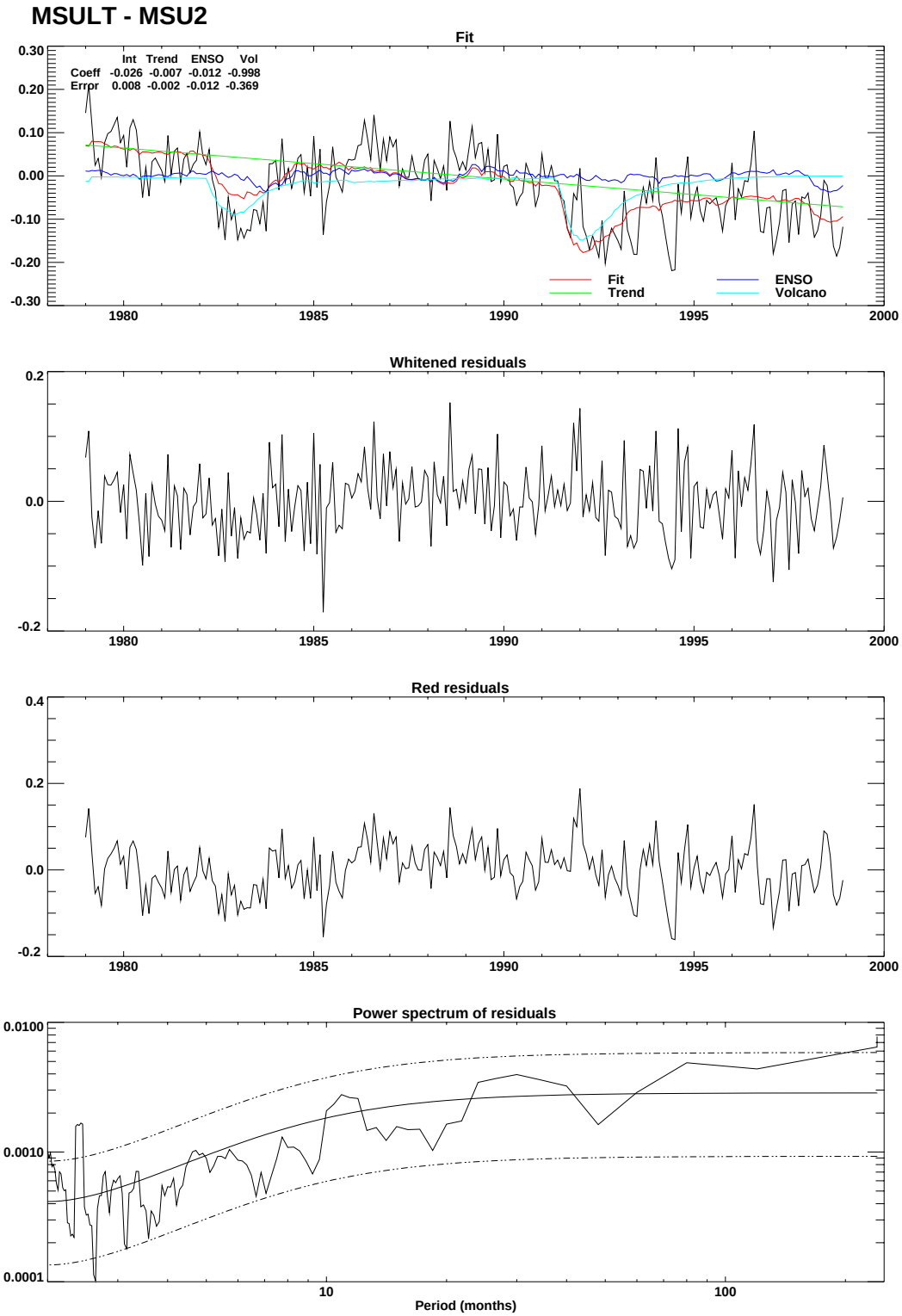

Figure 4b. As Fig. 2b, but for MSU2LT minus MSU2.

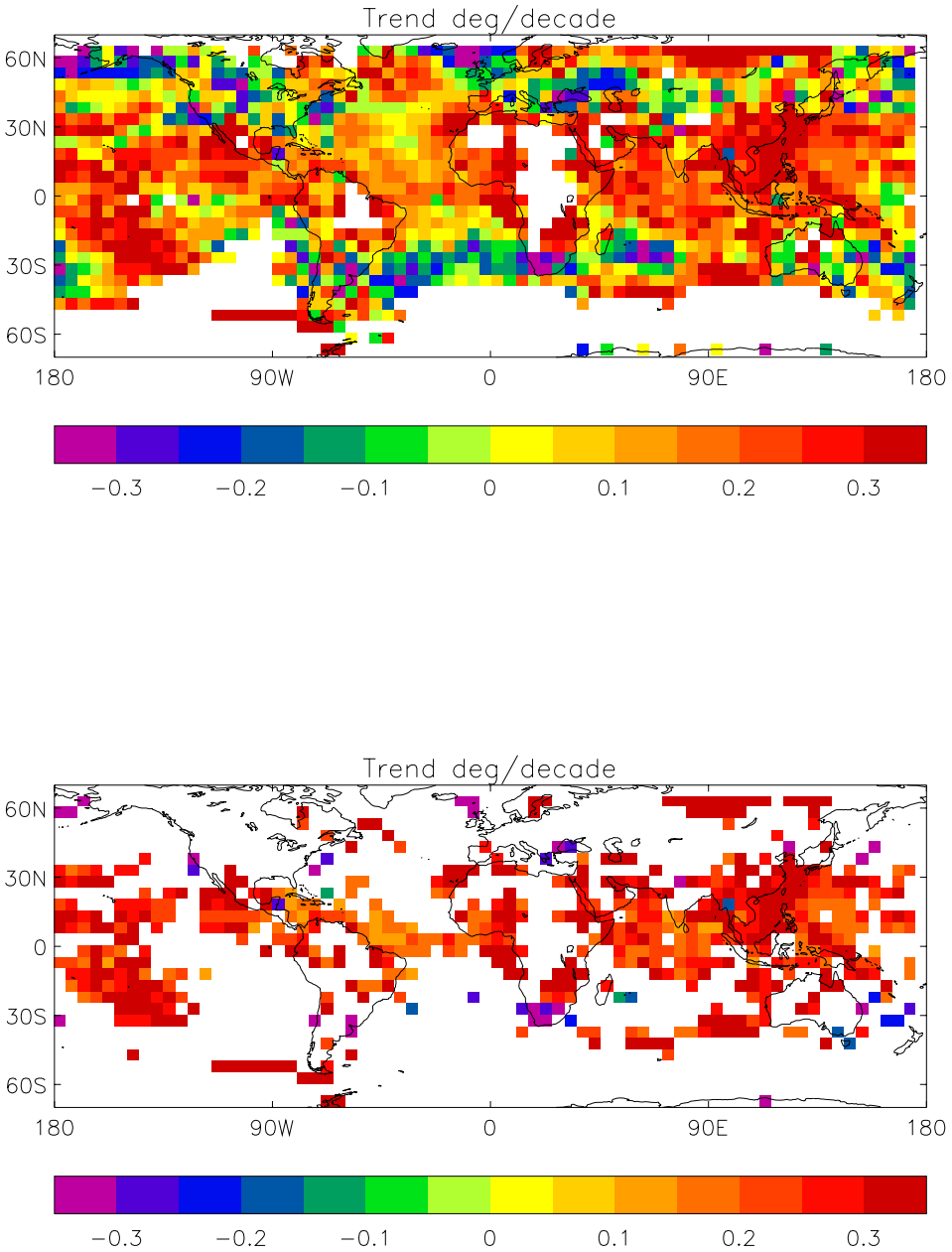

Figure 5a. Field of REML trends of JONES/MOHSST minus MSULT (JMLT). Monthly series for 1979-1998 for each grid box were subtracted, and REML regression with first-order autoregression term was then used to estimate, simultaneously, intercept, linear trend and the influences of ENSO and volcanic eruptions. The upper panel show trends (deg/decade) for all grid boxes with <30% of data missing. The lower panels shows only those grid boxes where the fitted trend was significant at the 95% level.

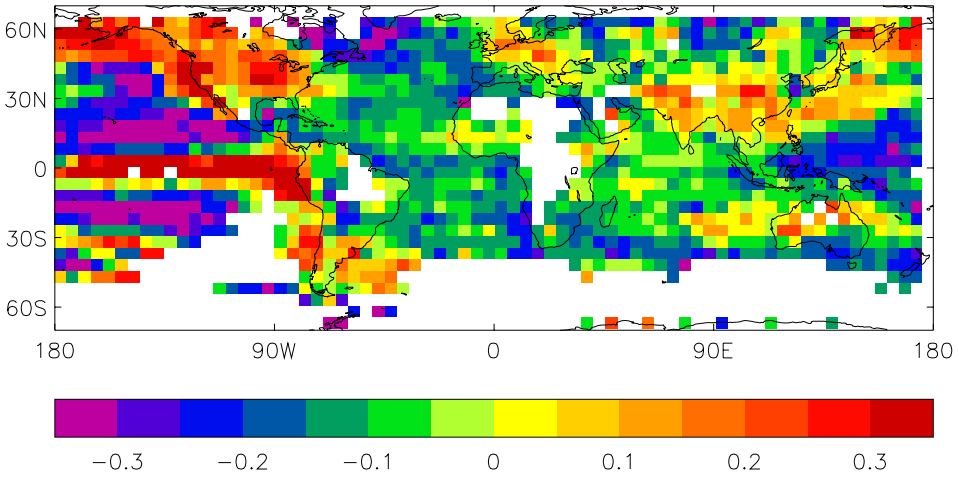

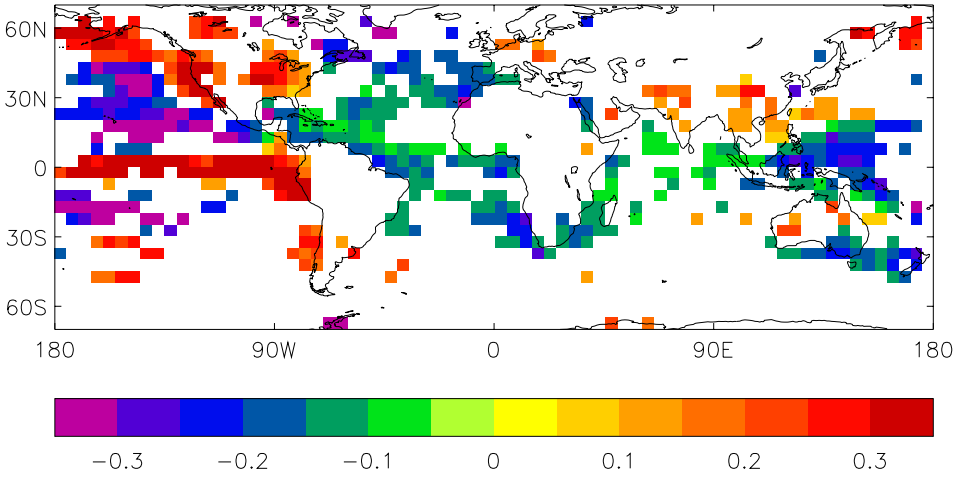

Figure 5b. As Fig. 5a but for the ENSO coefficient. Units are as for Table 1.

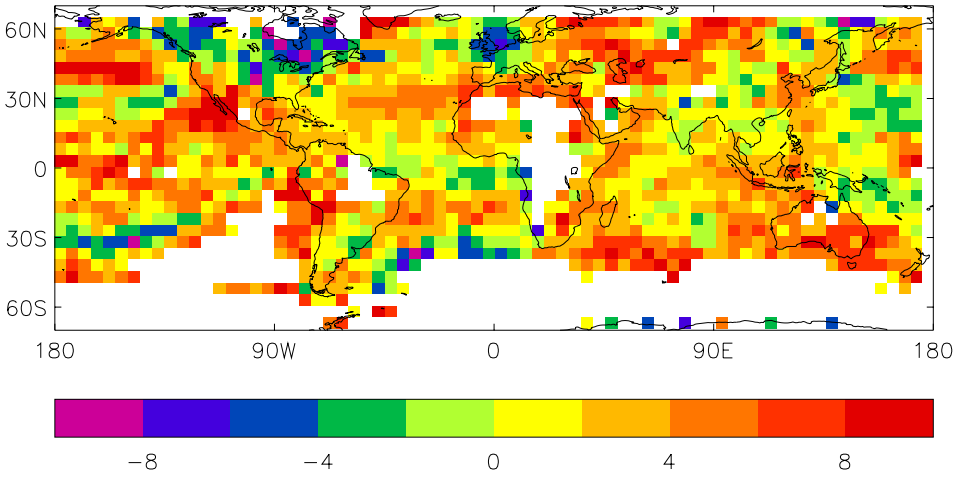

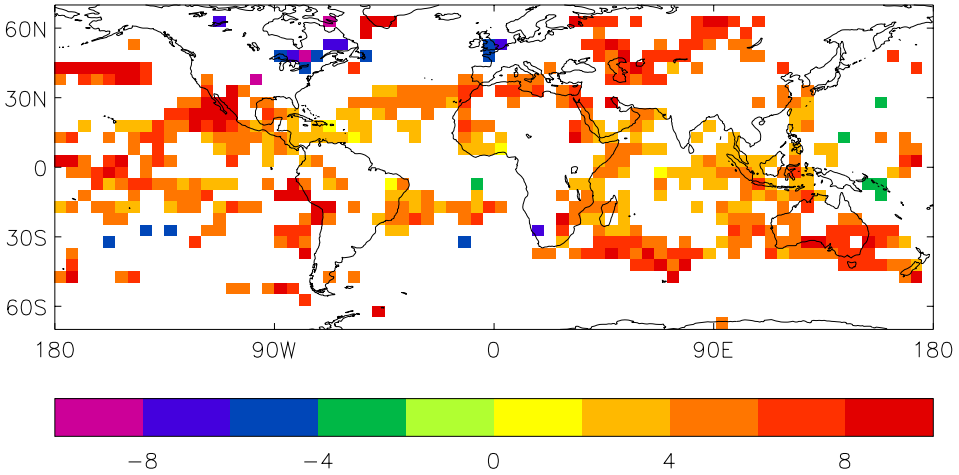

Figure 5c. As Fig. 5a but for the volcanic coefficient. Units are as for Table 1.

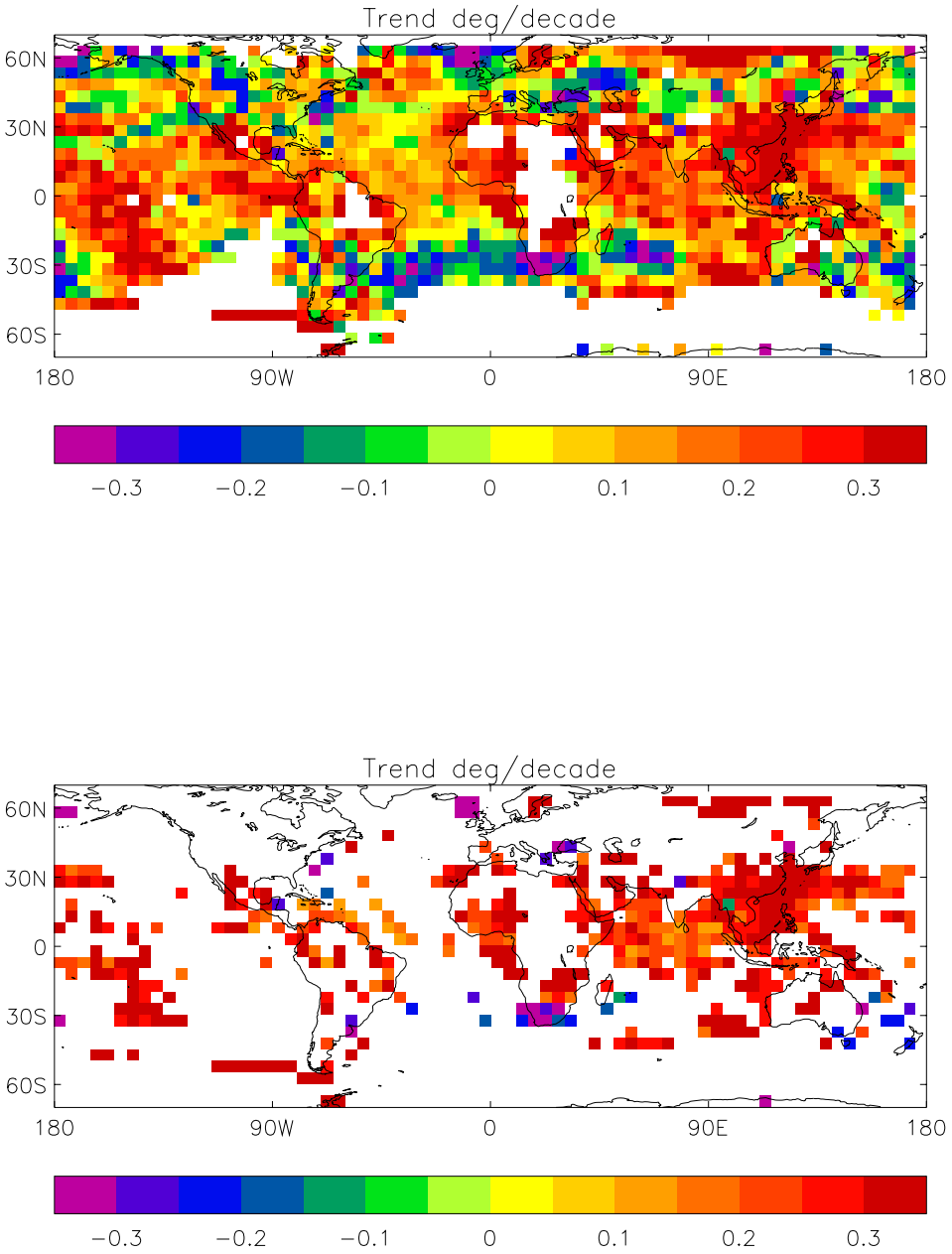

Figure 5d. As Fig. 5a but using REML to estimate trend alone.